Progress in Oceanography 161 (2018) 1–18

Contents lists available at ScienceDirect

Progress in Oceanography

journal homepage: www.elsevier.com/locate/pocean

Predictability and environmental drivers of chlorophyll fluctuations vary across different time scales and regions of the North Sea

Anouk N. Blauw[a,b,*], Elisa Benincà[a,d], Remi W.P.M. Laane[a,b,1], Naomi Greenwood[c], Jef Huisman[a]

[a] Department of Freshwater and Marine Ecology, Institute for Biodiversity and Ecosystem Dynamics, University of Amsterdam, Amsterdam, The Netherlands
[b] Marine and Coastal Systems, Deltares, Delft, The Netherlands
[c] Environment and Ecosystems, Centre for Environment, Fisheries and Aquaculture Science (CEFAS), Lowestoft, Suffolk, United Kingdom
[d] Centre for Zoonoses and Environmental Microbiology, National Institute for Public Health and the Environment, Bilthoven, The Netherlands

ARTICLE INFO

Keywords:
Marine monitoring
Mooring buoys
Particle settling
Phytoplankton
Tidal mixing
Time series analysis
North Sea, predictability, Generalized Additive Model

ABSTRACT

Phytoplankton concentrations display strong temporal variability at different time scales. Recent advances in automated moorings enable detailed investigation of this variability. In this study, we analyzed phytoplankton fluctuations at four automated mooring stations in the North Sea, which measured phytoplankton abundance (chlorophyll) and several environmental variables at a temporal resolution of 12–30 min for two to nine years. The stations differed in tidal range, water depth and freshwater influence. This allowed comparison of the predictability and environmental drivers of phytoplankton variability across different time scales and geographical regions. We analyzed the time series using wavelet analysis, cross correlations and generalized additive models to quantify the response of chlorophyll fluorescence to various environmental variables (tidal and meteorological variables, salinity, suspended particulate matter, nitrate and sea surface temperature). Hour-to-hour and day-to-day fluctuations in chlorophyll fluorescence were substantial, and mainly driven by sinking and vertical mixing of phytoplankton cells, horizontal transport of different water masses, and non-photochemical quenching of the fluorescence signal. At the macro-tidal stations, these short-term phytoplankton fluctuations were strongly driven by the tides. Along the Dutch coast, variation in salinity associated with the freshwater influence of the river Rhine played an important role, while in the central North Sea variation in weather conditions was a major determinant of phytoplankton variability. At time scales of weeks to months, solar irradiance, nutrient conditions and thermal stratification were the dominant drivers of changes in chlorophyll concentrations. These results show that the dominant drivers of phytoplankton fluctuations differ across marine environments and time scales. Moreover, our findings show that phytoplankton variability on hourly to daily time scales should not be dismissed as environmental noise, but is related to vertical and horizontal particle transport driven by winds and tides. Quantification of these transport processes contributes to an improved predictability of marine phytoplankton concentrations.

1. Introduction

Environmental drivers of phytoplankton fluctuations can be different at different temporal scales. Interannual variability and decadal trends in phytoplankton concentrations are often related to climatic variation and/or changes in the eutrophication status of marine waters (e.g., Breton et al., 1996; Gonzalez et al., 2000; Belgrano et al., 1999; Ottersen et al., 2001; Richardson and Schoeman, 2004; McQuatters-Gollop and Vermaat, 2011). At seasonal time scales, the annual cycles of solar irradiance and air temperature, and associated changes in thermal stratification, nutrient availability and grazing are often major drivers of the dynamics and succession of phytoplankton (Sverdrup, 1953; Sharples et al., 2006; Winder and Cloern, 2010; Sommer et al., 2012). At short time scales ranging from seconds to minutes (the inertial subrange) phytoplankton populations tend to follow small-scale variation in turbulent mixing as passive tracers (Kolmogorov, 1941; Franks, 2005).

Environmental drivers of phytoplankton fluctuations differ not only between time scales, but also between marine environments. Yet, only few studies have compared patterns of phytoplankton variability across ecosystems. In particular, Cloern and Jassby (2010) investigated seasonal and interannual variability of 84 estuarine and coastal sites, and

Abbreviations: GAM, Generalized Additive Model; PAR, Photosynthetically Active Radiation; SPM, Suspended Particulate Matter; SST, Sea Surface Temperature

* Corresponding author at: Deltares, P.O. Box 177, 2600 MH Delft, Netherlands.
E-mail address: anouk.blauw@deltares.nl (A.N. Blauw).

[1] Deceased May 31, 2016.

https://doi.org/10.1016/j.pocean.2018.01.005
Received 26 October 2017; Accepted 11 January 2018
Available online 12 January 2018

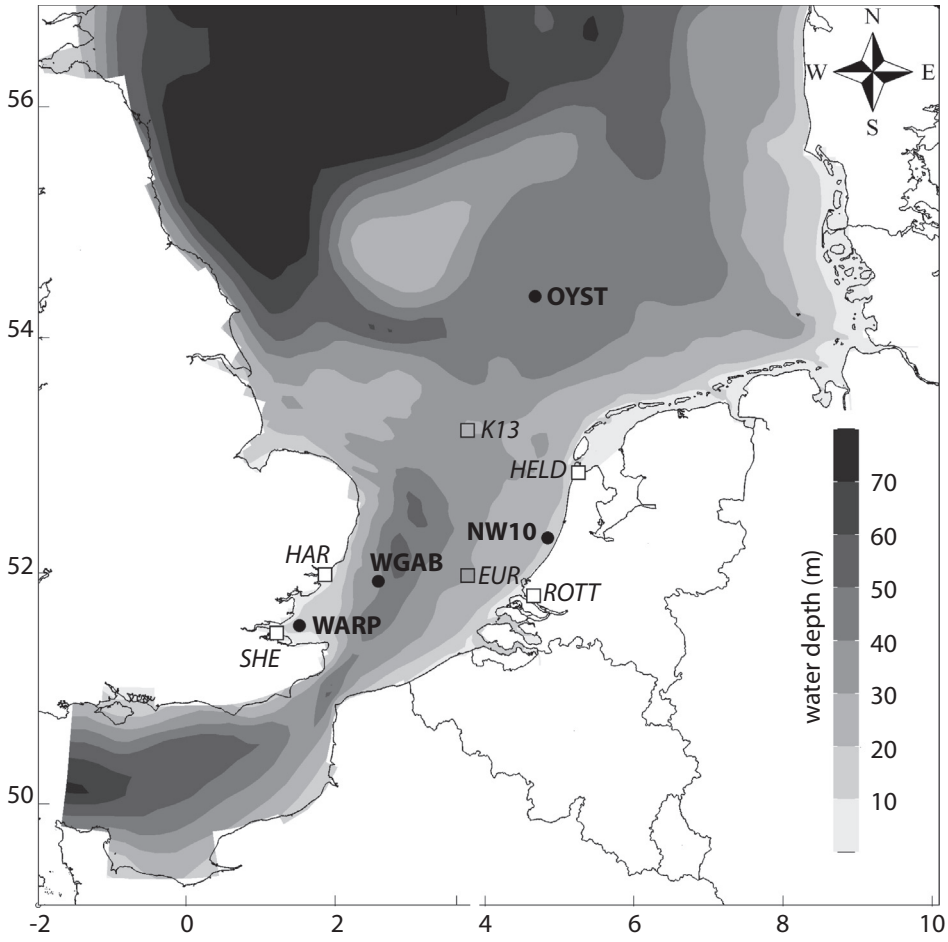

Fig. 1. Location of the monitoring stations. Map of the southern North Sea with the mooring stations (circles) and stations where supporting measurements of weather and tides have been made (open squares). Phytoplankton data were obtained from Smartbuoys at mooring stations Warp (WARP), West-Gabbard (WGAB), Noordwijk 10 km (NW10) and Oystergrounds (OYST). Tidal data were obtained from tide gauges at stations Sheerness (SHE), Harwich (HAR), NW10 and K13. Meteorological data were obtained from stations Europlatform (EUR), Den Helder (HELD), Rotterdam (ROTT), NW10 and K13.

this was further extended by Winder and Cloern (2010) to include time series of lakes and open oceans. Their analyses provided many new insights, and revealed large differences across ecosystems. Some ecosystems were dominated by recurrent seasonal patterns while other ecosystems showed large year-to-year variability. However, these studies mainly focused on seasonal and interannual variation, whereas phytoplankton fluctuations at shorter time scales were either not monitored at a sufficient temporal resolution or disregarded as residual events (Cloern and Jassby, 2010; Winder and Cloern, 2010).

Yet, a better understanding of phytoplankton fluctuations at time scales of hours to weeks may help to interpret the variability observed in phytoplankton time series and may improve forecasts of phytoplankton bloom development. Phytoplankton populations have specific growth rates of 0.1–2 day^{-1}. Phytoplankton fluctuations that are faster than the typical time scales of phytoplankton growth cannot be explained by variation in growth rates, but are likely to have their origins in physical transport of phytoplankton cells by, e.g., wind-induced mixing or tidal currents (Harris, 1980; Denman and Gargett, 1995; Mann and Lazier, 2009).

The important role of these physical transport processes is apparent in our earlier analysis of time series data monitored by an automated mooring station in the southern North Sea, which revealed that the phytoplankton concentration fluctuated at tidal periodicities of 6 h 12 min, 12 h 25 min, and 15 days (Blauw et al., 2012). A periodicity of 6 h 12 min reflects the typical periodicity of tidal current speeds, which causes resuspension of phytoplankton cells and other particles during periods with high tidal current speeds (between each high and low tide) and settlement of these particles at the tidal slacks. A periodicity of 12 h 25 min reflects horizontal displacement of water masses with different phytoplankton concentrations by the semidiurnal tidal cycle, while a periodicity of 15 days reflects variation in tidal energy by the spring-neap tidal cycle. Interestingly, spring blooms in these coastal waters slowly build up over several spring-neap tidal cycles, and subsequently expand in late spring when a strong decline of the SPM concentration during neap tide provides a temporary window for rapid growth of the phytoplankton population (Blauw et al., 2012).

However, these patterns are likely to be specific for macro-tidal coastal waters. In the central North Sea the tidal amplitude is lower and the water column can be strongly stratified. Here, tidal-induced mixing will be less important, but wind-induced mixing, convective cooling and other forms of weather-related variation can have a large impact on the day-to-day phytoplankton fluctuations. For instance, van Haren et al. (1998) found that the onset of stratification in early summer caused a decline in the near-surface phytoplankton concentration due to settling diatoms and a concomitant increase of the phytoplankton population in deeper water layers. This deeper population served as a source for temporary increases in the surface layer during episodic events with intensified turbulence due to storms, which brought part of the diatom population back upward.

In this study, we investigate the hypothesis that the relative importance of different environmental drivers and the overall predictability of phytoplankton fluctuations varies across different time scales and geographical regions. More specifically, we hypothesize that phytoplankton populations will essentially behave as passive tracers or particles at short (hour-to-hour) time scales where physical transport processes will dominate phytoplankton variability. Conversely, biological growth and loss processes will be important at longer (week-to-week) time scales. At intermediate (day-to-day) time scales phytoplankton fluctuations will be governed by the interplay between these physical and biological processes.

To investigate this hypothesis, we compare the chlorophyll fluctuations at four automated mooring stations in the North Sea. These four stations differ in their tidal range, water depth and degree of river influence. Our strategy is to decompose the time series by separating the observed phytoplankton fluctuations into three different time scales; hourly, daily and biweekly variation. We first calculated wavelet power spectra to identify distinct periodicities in the chlorophyll fluctuations. Subsequently, we related the chlorophyll fluctuations with a range of potentially important environmental variables (e.g., tidal range, wind speed, sea surface temperature, solar irradiance, nutrients) using cross correlation analysis. Finally, we integrated these environmental variables into generalized additive models, to assess the relative importance of different environmental drivers and overall predictability of phytoplankton variability between stations and between time scales.

2. Methods

2.1. Description of study sites

We analyzed data from four mooring stations in the North Sea (Fig. 1). The main characteristics of these mooring stations are summarized in Table 1. Station Warp (WARP) is located in the outer Thames estuary. In comparison to the other mooring stations, it has the shallowest water depth and the largest tidal range of 4.3 m. Station West-Gabbard (WGAB) is located about 40 km offshore from the English coast, and has an average tidal range of 3.2 m. Due to tidal mixing, both WARP and WGAB are not stratified during summer. Station Noordwijk 10 (NW10) is located 10 km offshore from the Dutch coastal town of Noordwijk, in the region of freshwater influence (ROFI) of the river Rhine. Water depth at this station is 18 m and the tidal range is 1.9 m. The interplay between freshwater inputs from the river Rhine and variable mixing intensity by weather and tides causes intermittent salinity stratification at NW10 (Simpson et al., 1993; De Ruijter et al., 1997; de Boer et al., 2009). Station Oystergrounds (OYST) is located in the central North Sea. It is the deepest station (45 m) with the smallest tidal range (1.5 m). During summer, station OYST is thermally stratified and a deep chlorophyll maximum may develop (van Haren et al., 1998; Weston et al., 2005).

Table 1
Main characteristics (± s.d) of the four mooring stations. Winter values are based on mooring data of January-February; summer values on those of July-August.

	Monitoring stations			
	WARP	WGAB	NW10	OYST
Coordinates (N, E)	51.31; 1.02	51.59; 2.05	52.18; 4.18	54.25; 4.02
Years analyzed	2001–2009	2002–2009	2000–2001	2006–2009
Water depth (m)	15	32	18	45
Tidal range (m)	4.3	3.2	1.9	1.4
Tidal gauge[a]	Sheerness	Harwich	NW10	K13
Salinity				
Winter	33.7 ± 1.0	35.0 ± 0.2	29.0 ± 2.2	34.8 ± 0.1
Summer	34.2 ± 0.4	34.8 ± 0.2	30.0 ± 1.3	34.7 ± 0.2
SPM (mg L^{-1})				
Winter	33.6 ± 15.0	13.0 ± 5.1	5.6 ± 3.1	2.5 ± 1.5
Summer	16.9 ± 17.1	5.3 ± 2.0	3.7 ± 4.4	0.3 ± 0.2
SST (°C)				
Winter	6.1 ± 1.3	7.9 ± 1.3	5.5 ± 0.6	6.8 ± 1.2
Summer	18.6 ± 1.0	17.4 ± 1.1	18.3 ± 1.2	16.8 ± 1.3
Nitrate (mmol m^{-3})				
Winter	29.3 ± 11.7	9.5 ± 2.2	54.5 ± 16.2	4.0 ± 1.7
Summer	4.7 ± 3.2	2.4 ± 1.7	9.2 ± 7.1	0.5 ± 0.3
Chlorophyll (mg m^{-3})				
Winter	1.1 ± 0.5	0.6 ± 0.2	0.5 ± 0.1	0.4 ± 0.1
Summer	4.3 ± 2.5	2.1 ± 0.9	4.4 ± 2.8	0.6 ± 0.3

[a] The nearest tidal gauge station used for data of tidal range; see Fig. 1 for locations.

2.2. Automated measurements

At each mooring station an automated measuring buoy, called a 'SmartbBuoy', has been deployed as part of the monitoring programs of the United Kingdom and The Netherlands (Mills et al., 2003). The SmartBuoys measured chlorophyll fluorescence, optical backscatter, salinity, temperature and photosynthetically active radiation (PAR) at 1 m depth, using sampling intervals ranging from 12 to 30 min. Nitrate concentrations were sampled at larger intervals, ranging from 1 to 4 h by the automated SmartBuoys at stations WARP and WGAB, from 1 to 4 days by the autosampler at OYST and from 15 to 60 days by sampling from a ship at stations NW10 and OYST.

Chlorophyll fluorescence was measured with a Seapoint fluorometer (Seapoint Inc.), and optical backscatter with a Seapoint turbidity meter (Seapoint Inc.). Fluorescence and optical backscatter were converted to concentrations of chlorophyll and suspended particulate matter (SPM), respectively, by calibration against chlorophyll and SPM concentrations measured in water samples taken during monthly service visits to the mooring stations. Although chlorophyll fluorescence is a very convenient measurement technique, it is known that the fluorescence signal can be quenched when cells are exposed to high light (Kiefer, 1973; Brunet and Lizon, 2003). This may cause a reduction in chlorophyll fluorescence during the daytime, especially in clear waters during sunny days.

Salinity and temperature were measured using an FSI CT sensor (Falmouth Scientific Inc.). Downwelling PAR was measured using a LiCor (LI-192) underwater quantum sensor (LiCor Biosciences). The concentration of total oxidised nitrogen (hereafter referred to as nitrate) was measured with a NAS-3X nutrient analyzer (EnviroTech). The SmartBuoy data can be downloaded or requested at the website https://www.cefas.co.uk/cefas-data-hub/smartbuoys/. Further details on the measurement methods and deployment of the SmartBuoys can be found in Greenwood et al. (2010). Seasonal phytoplankton dynamics and biogeochemistry have been described for station WARP (Weston et al., 2008) and station OYST (Greenwood et al., 2010). The impact of the tidal cycle on phytoplankton fluctuations at station WARP has been described by Blauw et al. (2012).

2.3. Tidal and meteorological data

Tidal and meteorological data were not measured by the SmartBuoys, but were obtained from the nearest tidal and meteorological stations. Tidal data were obtained from tide gauges at coastal stations Sheerness (SHE) and Harwich (HAR) and at the marine platforms K13 and NW10 (Fig. 1). The tide gauges measured sea water levels at 10 min intervals. The tidal range was calculated as the difference between the maximum and minimum water level of each day.

Meteorological data for daily averaged wind speed and air temperature were obtained from stations Europlatform (EUR) and K13A (K13), as provided at http://eca.knmi.nl (Klein Tank et al., 2002). Data on solar irradiance were obtained from stations De Kooy (near Den Helder: HELD) and Rotterdam (ROTT), as provided at http://www.knmi.nl/klimatologie/uurgegevens. We used meteorological data from K13 and HELD for OYST, and data from EUR and ROTT for the other three mooring stations.

2.4. Time scale decomposition

We applied time scale decomposition to separate the analysis of the observed phytoplankton fluctuations at three different time scales. Fig. 2 illustrates the steps taken to preprocess the data. First, we log-transformed the time series of chlorophyll and SPM (using the natural logarithm) to stabilize the variance and reduce the power of large peaks, such as the spring bloom. Then we calculated hourly and daily averages of the time series (black dots and blue line, respectively, in Fig. 2A). For the daily averages we included only measurements made

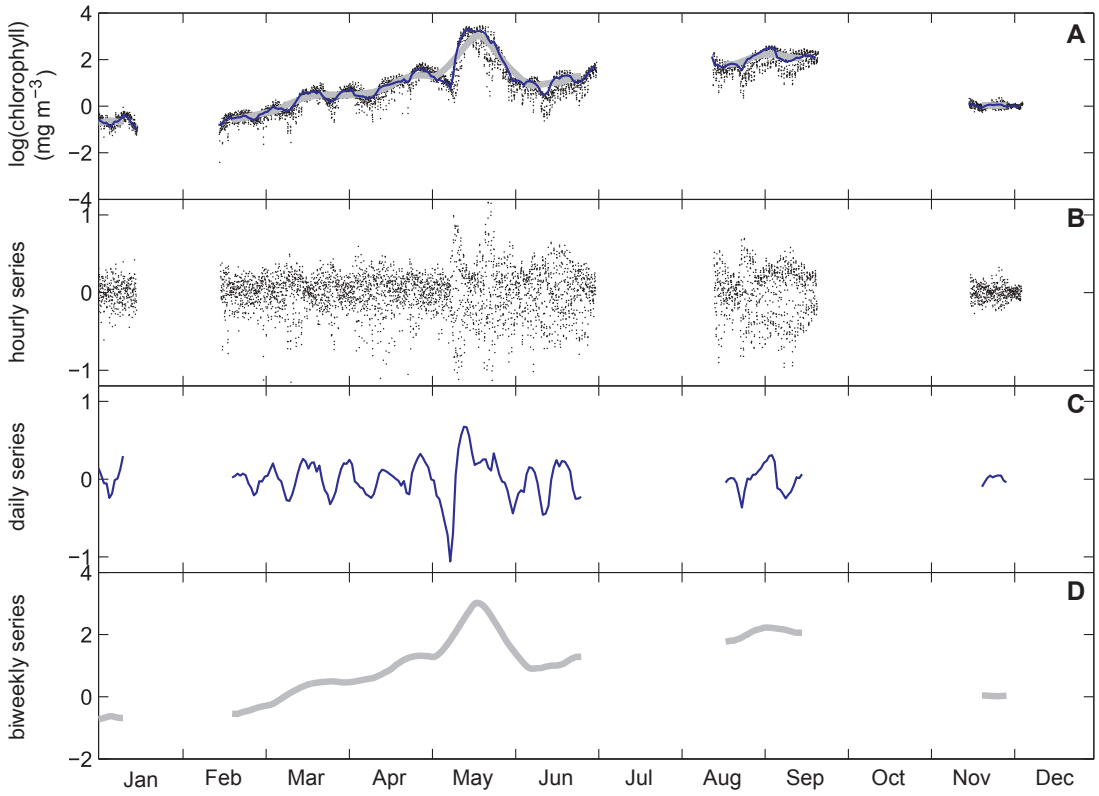

Fig. 2. Time scale decomposition. (A) Time series of the log-transformed chlorophyll concentration, with hourly-averaged data (dots), daily-averaged data (blue line) and the 15-day moving average (grey line). (B) The 'hourly time series', calculated as the deviation of the hourly-averaged from the daily-averaged data. (C) The 'daily time series', calculated as the deviation of the daily-averaged data from the 15-day moving average. (D) The 'biweekly time series', which is represented by the 15-day moving average. (For interpretation of the references to colour in this figure legend, the reader is referred to the web version of this article.)

in the dark (i.e., when observed PAR at 1 m depth was < 1 µmol quanta $m^{-2} s^{-1}$), to remove effects of non-photochemical quenching of the chlorophyll fluorescence. We also calculated the 15-day moving average of the daily averages (grey line in Fig. 2A).

We subtracted the daily from the hourly averages to obtain a detrended time series of the hour-to-hour fluctuations within the day. This will be referred to as the "hourly time series" (Fig. 2B). Subtracting the 15-day moving average from the daily averages produced a detrended time series of the day-to-day fluctuations (Fig. 2C). This "daily time series" enables analysis of phytoplankton fluctuations associated with the spring-neap tidal cycle. The 15-day moving average was used for the analysis of phytoplankton variability at the seasonal time scale, and is referred to as the "biweekly time series" (Fig. 2D).

2.5. Wavelet analysis

We applied wavelet analysis to investigate significant periodicities in the hourly and daily time series of chlorophyll (Fig. 2B and C). Wavelet analysis is a type of spectral analysis that is particularly suitable for the analysis of non-stationary time series, such as many ecological time series (Torrence and Compo, 1998; Cazelles et al., 2008). Local and global wavelet spectra of the chlorophyll fluctuations at station WARP have been presented previously (Blauw et al., 2012). Here we compare global wavelet spectra of the four different stations, using the same methodology as in Blauw et al. (2012). The statistical significance of periodicities revealed by wavelet analysis was tested by comparing the wavelet power spectrum of the observed time series against the 95% confidence level of wavelet power spectra generated by red noise, using an autoregressive AR1 model with the same autocorrelation coefficient as the observed time series. Reliable detection of a given periodicity with wavelet analysis requires uninterrupted time series that exceed ~4 times that periodicity (Cazelles et al., 2008). Due to gaps in the data sets, uninterrupted time series of sufficient length were not available for a sound wavelet analysis of the biweekly time series. The Matlab scripts for wavelet analysis, including significance tests, were developed by Torrence and Compo (1998) and Grinsted et al. (2004) (http://noc.ac.uk/using-science/crosswavelet-wavelet-coherence).

2.6. Cross correlations

We applied cross-correlation analysis to investigate relationships between the chlorophyll fluctuations and the measured environmental variables. Cross-correlation analysis calculates the Pearson's correlation coefficient (r) between two time series at different time lags. For this purpose, we first shifted the two time series with the time lag of interest. Subsequently, we removed all data pairs for which at least one of the data points was missing, and calculated the correlation coefficient for the remaining data pairs. This procedure was repeated for all time lags. If the correlation coefficient peaks at a time lag of 0, chlorophyll responds immediately to fluctuations in an environmental variable. If it peaks at a negative time lag, chlorophyll fluctuations follow fluctuations in an environmental variable with some delay. Cross-correlation analysis was applied to both the hourly and daily time series. The limited length prevented a sound cross correlation analysis of the biweekly time series.

The time series showed considerable autocorrelation. Therefore, we applied a Monte Carlo method to assess the statistical significance of the cross correlations. We used 1000 pairs of surrogate time series to estimate the distribution and 95% confidence interval of cross correlation coefficients based on red noise. These surrogate time series were generated with an AR1 model with random error and had the same sample size, mean, variance and lag-1 autocorrelation coefficient as the original time series.

2.7. Generalized Additive models

Finally, we investigated how much of the chlorophyll variability can be explained by the combined effects of the different environmental variables using Generalized Additive Models (GAMs) (Hastie and Tibshirani, 1990; Wood, 2006). GAMs are non-parametric regression models, where the relations between the response variable and the explanatory variables are represented by smooth functions. A key advantage of this approach is that GAMs do not require *a priori* specification of mathematical equations describing the presumed relationships, because the general shape of these relationships is captured by the smooth functions. GAMs were fitted to the hourly, daily, and biweekly time series using the mgcv package version 1.7–22 (Wood, 2006) of R version 3.01. The smooth functions were constructed as cubic splines and their optimal shape was estimated by minimizing the general cross validation (GCV) criterion. To limit the risk of overfitting we reduced the number of knots in the smooth functions to three.

For the hourly time series, the structure of the GAM model was:

$$P_{h,t} = b_h + \sum_{j=1}^{n} g_{h,j}(E_{h,j,t-lag}) + \varepsilon_{h,t}$$

where $P_{h,t}$ is the (log-transformed and detrended) chlorophyll concentration at time t, b_h is the intercept, $g_{h,j}(E_{h,j,t\text{-}lag})$ are smooth functions describing the effects of the (detrended) environmental variables $E_{h,1}$, …, $E_{h,n}$ at time t-*lag*, and $\varepsilon_{h,t}$ is a random error term. Similarly, for the daily time series, the structure of the GAM model was:

$$P_{d,t} = b_d + \sum_{j=1}^{n} g_{d,j}(E_{d,j,t-lag}) + \varepsilon_{d,t}$$

The lag time was set to zero, unless the cross-correlation analysis had identified a clear time delay between the chlorophyll fluctuations and the environmental variable. As environmental variables in the analysis of hourly and daily time series we used the cube of detrended wind speed as a proxy for wind mixing, salinity, solar irradiance (PAR), (log-transformed) SPM, sea surface temperature and air temperature (Table 2). In addition, we included a simple measure of tidal mixing intensity as an environmental variable. For the hourly time series, we calculated the (absolute) rate of change in water level as a proxy of tidal current speed (Blauw et al., 2012), and we used the cube of this tidal current speed as an indicator of tidal mixing intensity. For the daily time series, we used the cube of tidal range as an indicator of tidal mixing intensity (Blauw et al., 2012). Furthermore, we included nitrate as an environmental variable, but only for the daily time series of WARP and WGAB. The resolution of the nitrate data was insufficient for analyses at the hourly time scale and for NW10 and OYST also at the daily time scale.

Contrary to the hourly and daily time series, the biweekly time series was not detrended (Fig. 2). To improve stationarity, we therefore differenced the biweekly time series, i.e., we used the rate of change in chlorophyll as response variable in the GAM model. The rate of change was calculated from the difference between the (log-transformed) chlorophyll concentrations at time t and time t-1 day. The structure of the GAM model thus became:

$$P_{b,t} - P_{b,t-1} = b_b + \sum_{j} g_{b,j}(E_{b,j,t-1}) + \varepsilon_{b,t}$$

Because the chlorophyll concentrations were log-transformed, this equation describes the relative rate of change (i.e., the specific growth rate) of the phytoplankton population as a function of environmental variables. For the biweekly time series we used the same environmental variables as for the daily time series, except air temperature. Air temperature was removed, because it was strongly collinear with sea surface temperature in the biweekly time series. Nitrate was included for all stations, where we linearly interpolated the nitrate time series of NW10 and OYST to have sufficient data available for the analysis. In addition, we also included the rates of change of wind speed, sea surface temperature, salinity and SPM as environmental variables. Changes in these variables are indicative of changes in physical mixing and transport processes, which may result in changes in chlorophyll concentrations.

Residuals of the GAM models showed considerable autocorrelation at all three time scales, which could bias the significance tests. Therefore, we partitioned the time series in several subsets, by subsampling the time series at a sampling interval long enough to reduce the autocorrelation coefficient of the residuals. For the hourly time series, the autocorrelation coefficient of the residuals was reduced to $r < 0.2$ but remained significant even at sampling intervals over 24 h. Therefore, we subsampled the hourly time series every 7 h, so that the subsets did not repeatedly sample the same part of the 24-h day-night cycle or 25-h tidal cycle. For the daily time series, a sampling interval of 4 days was sufficient to remove the autocorrelation. For the biweekly time series, stations WARP, WGAB and NW10 were subsampled at an

Table 2
Overview of the GAM models at the different stations and time scales. Significant environmental variables are indicated by the number of subsets in which the variable was significant at $p < .05$; 'ns' indicates that the variable was not significant, and '–' indicates that the variable was not considered in the model analysis. N: number of datapoints per subset. R^2: adjusted R^2 of the GAM model for the complete time series.

Station	Total number of subsets	Environmental variables								N	R^2
		Tide[a]	Wind[b]	PAR	T Air	SST	Salinity	SPM	Nitrate		
Hourly time scale											
WARP	7	5	2	7	1	ns	3	7	–	3985	0.25
WGAB	7	7	4	7	5	7	7	7	–	3910	0.35
NW10	7	ns	ns	7	7	7	7	7	–	1311	0.32
OYST	7	ns	ns	7	6	7	ns	7	–	1019	0.51
Daily time scale											
WARP	4	ns	ns	Ns	Ns	ns	1	4	ns	191	0.15
WGAB	4	4	1	Ns	Ns	1	ns	ns	4	190	0.13
NW10	4	1	ns	Ns	1	ns	4	3	–	63	0.22
OYST	3	ns	ns	1	Ns	2	ns	ns	–	53	0.21
Biweekly time scale											
WARP	15	6	ns	8	–	Ns	2	13	ns	46	0.35
WGAB	15	1	1	6	–	6	8	ns	13	55	0.27
NW10	15	ns	ns	3	–	2	3	ns	12	16	0.45
OYST	8	ns	ns	6	–	4	5	6	7	18	0.63

[a] The cube of tidal current speed was used as proxy of tidal mixing
[b] The cube of wind speed was used as proxy of wind mixing.

interval of 15 days to remove the autocorrelation introduced by the 15-day smoothing. Because of missing values the number of data points per subset became too small for a meaningful analysis of station OYST when using a sampling interval of 15 days (i.e., the number of data points became similar to the number of explanatory variables to be fitted). We therefore subsampled the biweekly time series of station OYST at a shorter interval of 8 days. Consequently, temporal autocorrelation was reduced, but the data within the subsets of this time series were not strictly independent.

GAM models were fitted separately to each subset of the time series. We pruned the GAM models by stepwise removal of the environmental variable with highest *p*-value, until all environmental variables in the GAM model were significant at $p < 0.05$. The *p*-values were calculated according to Wood (2013). Subsequently, to aggregate all results, we fitted a GAM model to the complete time series using only those environmental variables that were significant in at least one of the subsets.

2.8. Predictability of chlorophyll

To assess the overall predictability of the chlorophyll fluctuations we reconstructed the chlorophyll time series predicted by the GAM models by adding up the GAM results for all three time scales (i.e., the opposite of the time scale decomposition in Fig. 2):

$$P_{r,t} = P_{b,t-1} + b_b + \sum_j g_{b,j}(E_{b,j,t-1}) + P_{d,t} + P_{h,t}$$

where $P_{r,t}$ is the reconstructed (log-transformed) chlorophyll concentration at time *t*. Starting from the biweekly averaged chlorophyll observations ($P_{b,t-1}$), we generated model predictions at an hourly resolution for lead times up to 30 days ahead. We calculated coefficients of determination (R^2) between the reconstructed hourly chlorophyll series and the observed chlorophyll series for each lead time. We compared these with the R^2 values of a null model that assumed that the chlorophyll concentration at time $t + 1$ h was the same as at time *t*. This null model shows how well chlorophyll concentrations can be predicted ahead by autocorrelation alone. The difference between the R^2 values of our model predictions and the null model is used to assess how much the predictability can be improved by including information about the environmental drivers of chlorophyll fluctuations.

3. Results and discussion

3.1. Time series

The time series of the mooring stations spanned several years (Table 1), and representative years of each of the four stations are illustrated in Figs. 3–6. The tidal range was higher at WARP and WGAB (Figs. 3A, 4A) than at NW10 and OYST (Figs. 5A, 6A). The chlorophyll fluctuations differed in frequency and amplitude between the stations. At WARP, the chlorophyll and SPM concentration showed a distinct 15-day periodicity associated with the spring-neap tidal cycle (Fig. 3B; see also Blauw et al., 2012). At WGAB, the chlorophyll and SPM concentrations fluctuated at a similar time scale, but less pronounced (Fig. 4B). NW10 showed chlorophyll and SPM fluctuations at shorter time scales of only a few days (Fig. 5B), and several troughs in the chlorophyll time series seemed to coincide with low salinity events, e.g., in April (Fig. 5D). The chlorophyll concentration at OYST varied strongly within the day, but showed less day-to-day variation than the other stations (Fig. 6B).

Spring blooms occurred in May at WARP and WGAB (Figs. 3B, 4B), and in April at OYST (Fig. 6B). At all three stations, the onset of the spring bloom coincided with a sharp decrease in SPM concentration. Station NW10 did not show a distinct spring bloom, but rather a concatenation of blooms from March through June (Fig. 5B).

Nitrate concentrations dropped sharply during the spring blooms at WARP, WGAB and OYST (Figs. 3C, 4C, 6C). At NW10 the available data suggest a more gradual decrease in nitrate concentration during spring and summer (Fig. 5C). The chlorophyll concentrations during the spring bloom at WARP did not exceed those at WGAB, although winter nitrate concentrations at WARP were at least twice as high as at WGAB. Summer nitrate concentrations were depleted to a lesser extent at WARP and NW10 than at WGAB and particularly OYST (Table 1).

At WARP salinity fluctuated between 31 and 35 during winter and early spring, indicative of intermittent higher river discharges from the Thames in winter, while salinity remained fairly constant during the remainder of the year (Fig. 3D). At NW10, salinity showed large fluctuations throughout the year, with occasional declines down to 20 during winter and spring, indicative of the strong freshwater influence of the river Rhine (Fig. 5D). At stations WGAB and OYST salinity remained largely between 34 and 35 throughout the year, showing much less freshwater influence than the other two stations (Fig. 4D, 6D).

Sea surface temperature tracked air temperature at all four stations, with a smoother seasonal cycle at WARP and WGAB than at NW10 (Fig. 3D, 4D, 5D). Sea surface temperature at OYST showed a smooth seasonal cycle during most of the year, except during the build-up of thermal stratification where occasional declines in SST are indicative of episodic mixing events in early summer (Fig. 6D).

3.2. Dominant periodicities

Global wavelet spectra reveal that hourly averaged chlorophyll concentrations fluctuated with periodicities of 6 h 12 min, 12 h 25 min, and 24 h at all four stations (Fig. 7A, C, E, and G). The 6 h 12 min periodicity reflects the periodicity of the tidal current speed, which reaches maximum velocity during both the rise and the fall of the tides (i.e., two times per semi-diurnal tidal cycle). Strong tidal currents enhance turbulent mixing and thereby mix up phytoplankton cells, including large diatoms, from deeper water layers or from the sediment (Blauw et al., 2012). The 12 h 25 min periodicity reflects horizontal displacement of coastal waters by the semi-diurnal tidal cycle in areas with a cross-shore gradient of the chlorophyll concentration (e.g., due to freshwater inputs). The 24-h periodicity reflects the day-night cycle. The peaks in the global wavelet spectra exceed the 95% confidence level of red noise (dashed lines in Fig. 7), confirming the significance of these periodicities. For short periods an isolated patch of phytoplankton moving back and forth passing the mooring may also generate 6 h 12 min periodicity in chlorophyll concentrations. However, the consistent 6 h 12 min periodicity over long time periods throughout the 9-year time series indicates that it is unlikely that this periodicity can be attributed to isolated phytoplankton patches, since these would not be persistent at the same location.

The relative importance of the 6 h 12 min periodicity is largest at WARP, less prominent at station WGAB, and only minor at NW10 and OYST (Fig. 7A, C, E, and G). The 24 h periodicity shows the opposite pattern: it is dominant at OYST, less important at NW10, and relatively minor at WGAB and WARP. The 12 h 25 min periodicity is dominant at WGAB, less important at WARP and NW10, and only minor at OYST. These results indicate that resuspension of phytoplankton by high tidal current speeds is an important process at WARP and to some extent also at WGAB, but not at NW10 and OYST. Horizontal transport of water masses with different phytoplankton populations is particularly relevant at WGAB, whereas the day-night cycle plays a prominent role at station OYST in the central North Sea.

Global wavelet spectra of daily averaged chlorophyll concentrations show a dominant periodicity of 15 days at stations WARP and WGAB (Fig. 7B and D). This 15-day periodicity indicates that the phytoplankton fluctuations at these two macro-tidal stations are affected by the spring-neap tidal cycle, in line with earlier results of Blauw et al. (2012). In contrast, the phytoplankton populations at the microtidal stations NW10 and OYST show significant variability at time scales of 8–10 days, but do not fluctuate at the 15-day periodicity of the spring-

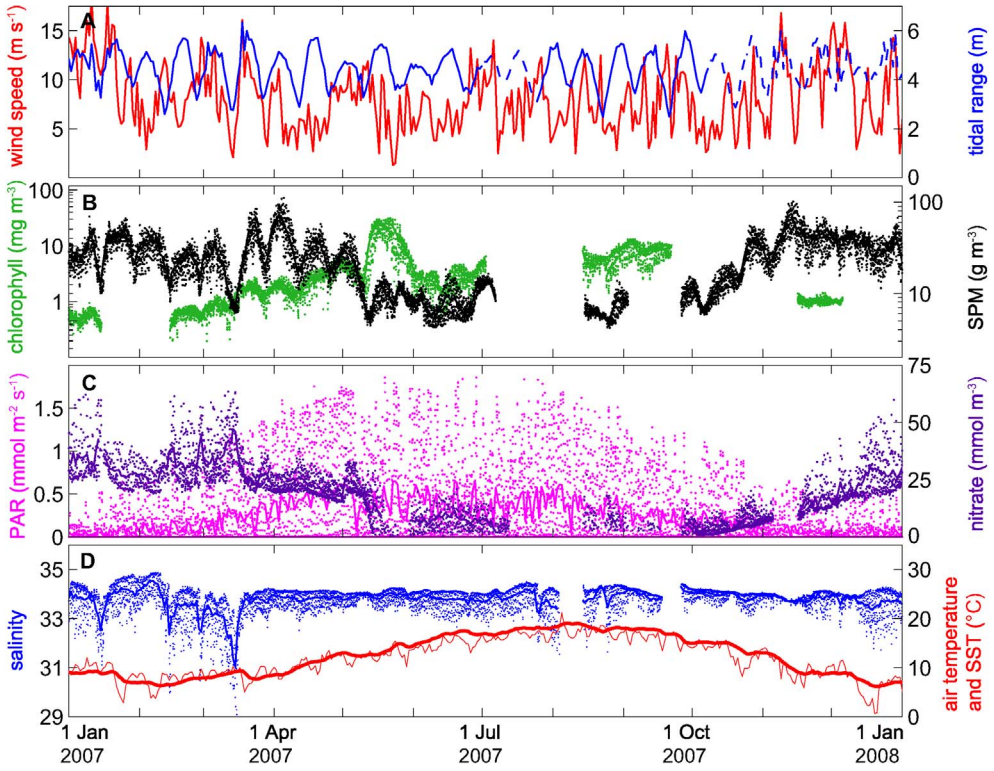

Fig. 3. Time series at WARP in 2007. (A) Wind speed (red line) and tidal range (blue solid line). Tidal data were obtained from station SHE (Sheerness); when tidal data at SHE were missing, we show the tidal range at station K13 (blue dashed line) rescaled to match the mean and amplitude of the tidal range at SHE. (B) Concentrations of chlorophyll (green) and SPM (black). (C) Nitrate concentration (dark purple) and irradiance (PAR, pink). (D) Salinity (blue), air temperature (thin red line) and sea surface temperature (bold red line). In (B-D), dots show the hourly averages and lines the daily averages. (For interpretation of the references to colour in this figure legend, the reader is referred to the web version of this article.)

neap tidal cycle (Fig. 7F and H).

3.3. Cross correlations of chlorophyll with environmental variables

The cross correlations revealed many significant relationships between the chlorophyll fluctuations and environmental variables (Figs. 8, 9). Cross correlations show the Pearson correlation coefficient (r) between a response variable (chlorophyll) and an explanatory variable at different time lags. If r is highest at a time lag of zero, the response is instantaneous. If it peaks at a negative time lag, there is a delay between fluctuations in the explanatory variable and corresponding fluctuations in chlorophyll. To focus the presentation, here we highlight those relationships that we regard as most relevant.

3.3.1. The tidal cycle

Cross correlations of the hourly averaged chlorophyll concentration

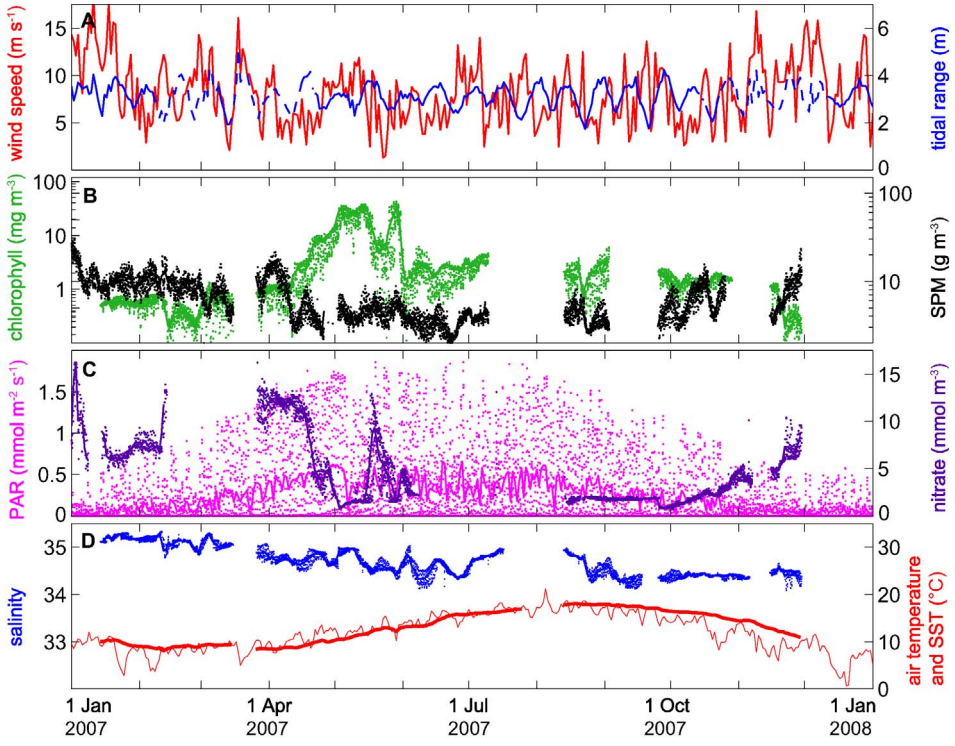

Fig. 4. Time series at WGAB in 2007. (A) Wind speed (red line) and tidal range (blue solid line). Tidal data were obtained from station HAR (Harwich); when tidal data at HAR were missing, we show the tidal range at station SHE or K13 (blue dashed line) rescaled to match the mean and amplitude of the tidal range at HAR. (B) Concentrations of chlorophyll (green) and SPM (black). (C) Nitrate concentration (dark purple) and irradiance (PAR, pink). (D) Salinity (blue), air temperature (thin red line) and sea surface temperature (bold red line). In (B-D), dots show the hourly averages and lines the daily averages. (For interpretation of the references to colour in this figure legend, the reader is referred to the web version of this article.)

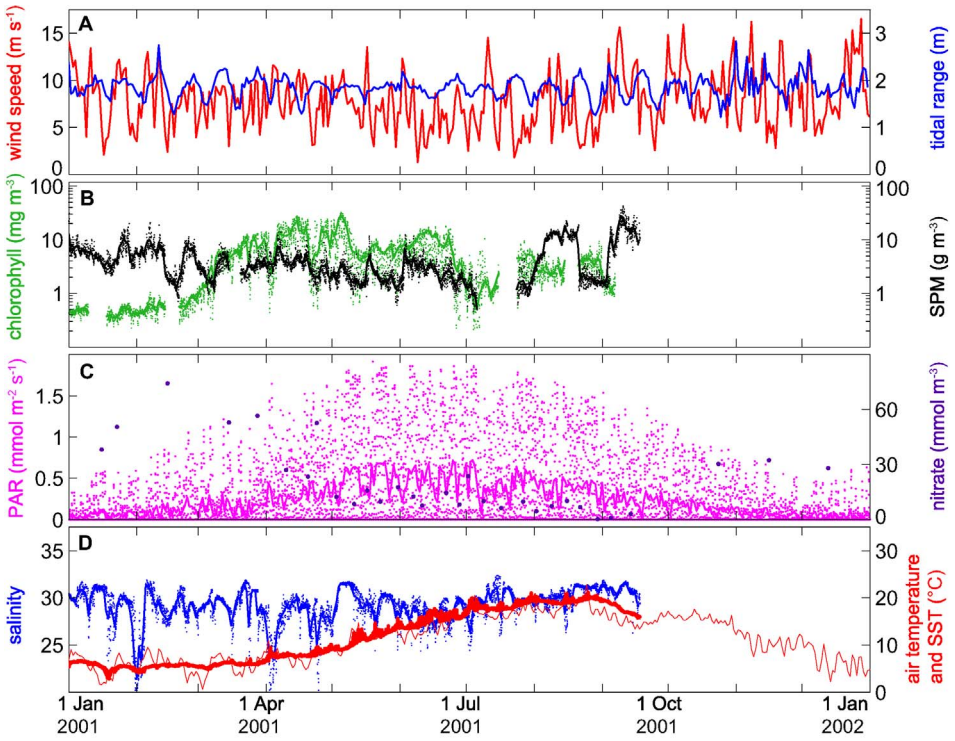

Fig. 5. Time series at NW10 in 2001. (A) Wind speed (red line) and tidal range (blue solid line). (B) Concentrations of chlorophyll (green) and SPM (black). (C) Nitrate concentration (large purple data points, sampled only once every 15 to 30 days) and irradiance (PAR, pink). (D) Salinity (blue), air temperature (thin red line) and sea surface temperature (bold red line). In (B-D), dots show the hourly averages and lines the daily averages. (For interpretation of the references to colour in this figure legend, the reader is referred to the web version of this article.)

with tidal current speed show a 6-h 12-min periodicity at both WARP and WGAB (Fig. 8A1 and A2). This periodicity confirms that phytoplankton fluctuations at both stations are strongly associated with fluctuations in tidal current speed, consistent with the global wavelet spectra in Fig. 7A and C. The cross correlations at both stations reveal a time-lag of 1 h between maximum tidal current speed and maximum chlorophyll concentration, indicating that the chlorophyll concentrations peaked slightly after the maximum tidal current speed was reached (Blauw et al., 2012). The cross correlations with tidal current speed are less pronounced and lack a 6-h 12-min periodicity at NW10 and OYST (Fig. 8A3 and A4). However, a 12-h 25-min and 24-h periodicity can be recognized at NW10 and a 24-h periodicity at OYST, consistent with the global wavelet spectra (Fig. 7E and G).

Cross correlations of the daily time series with tidal range showed a 15-day periodicity at WARP and WGAB (Fig. 9A1 and A2), consistent with the global wavelet spectra (Fig. 7B and D). The positive correlation at zero time lag indicates that chlorophyll fluctuated in phase with tidal range, with highest chlorophyll concentrations during spring tide and

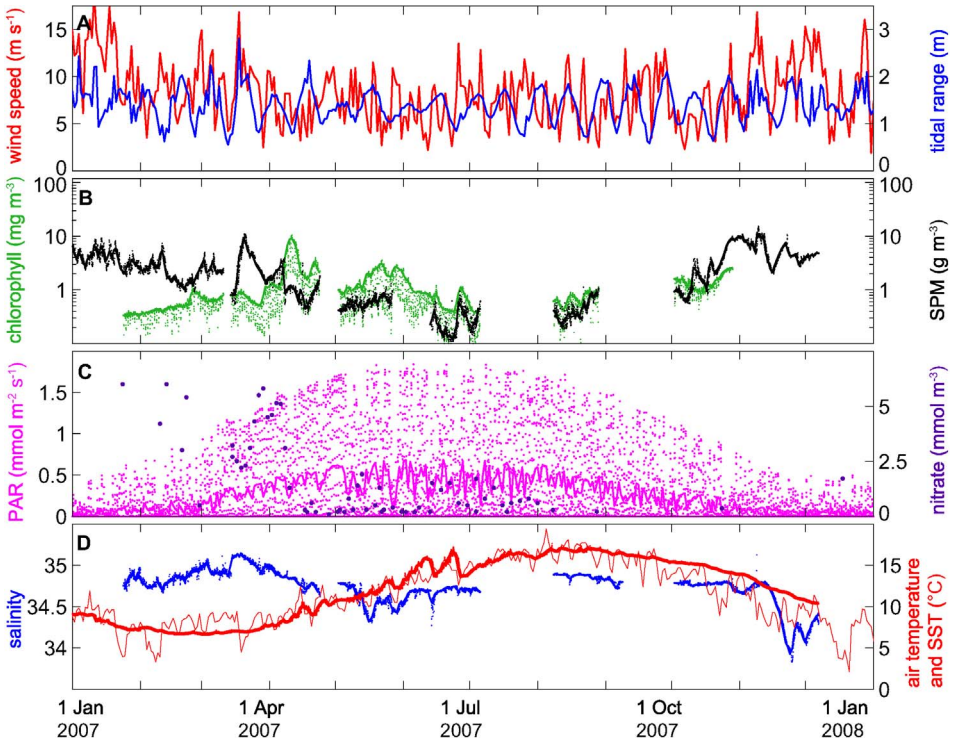

Fig. 6. Time series at OYST in 2007. (A) Wind speed (red line) and tidal range (blue solid line). Tidal data were obtained from station K13. (B) Concentrations of chlorophyll (green) and SPM (black). (C) Nitrate concentration (large purple data points, sampled only once every 1 to 60 days) and irradiance (PAR, pink). (D) Salinity (blue), air temperature (thin red line) and sea surface temperature (bold red line). In (B-D), dots show the hourly averages and lines the daily averages. (For interpretation of the references to colour in this figure legend, the reader is referred to the web version of this article.)

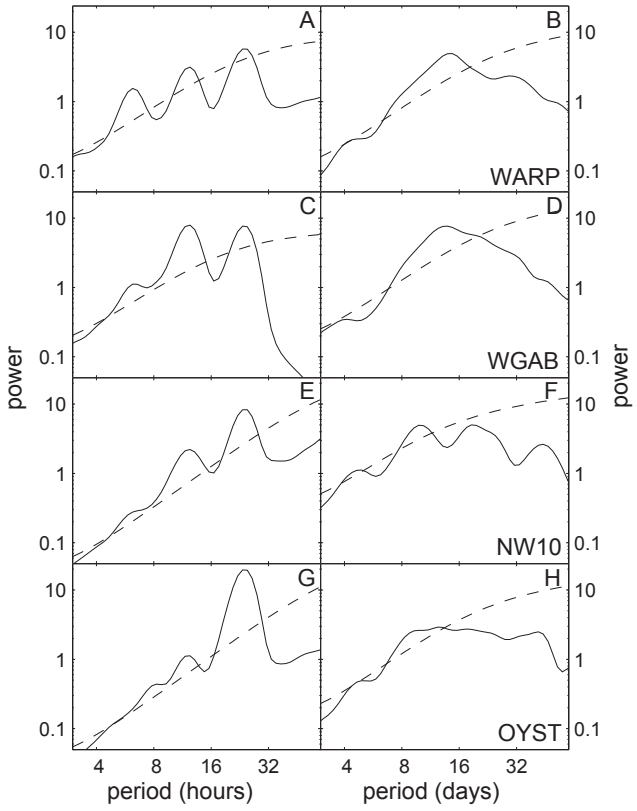

Fig. 7. Global wavelet power spectra of chlorophyll fluctuations. Global wavelet power spectra of chlorophyll fluctuations at the four mooring stations: (A,B) WARP. (C,D) WGAB. (E,F) NW10. (G,H) OYST. (A, C, E, G) show the spectra of the hourly time series, and (B, D, F, H) show the spectra of the daily time series. Peaks exceeding the 95% confidence level of the corresponding red noise spectra (dashed lines) are significant.

lowest during neap tide. Cross correlations with tidal range were not significant at NW10 and OYST (Fig. 9A3 and A4).

3.3.2. Wind speed

In the hourly time series, chlorophyll showed a positive cross correlation with wind speed at lag zero, with a 24-h periodicity at all four stations (Fig. 8B1-4). In the daily time series, chlorophyll showed a positive cross correlation with wind speed at lag zero at WARP and WGAB, and at a time delay of 1 day at OYST (Fig. 9B). Hence, elevated wind speeds were associated with elevated chlorophyll concentrations at all 4 stations.

3.3.3. Solar irradiance

In the hourly time series, cross correlations with surface PAR showed a 24-h periodicity with negative correlations around lag zero (Fig. 8C1-4). Hence, chlorophyll concentrations reached their daily minimum around midday. Similar results were reported by Van Haren et al. (1998), who measured chlorophyll concentrations at stations OYST by both fluorescence and HPLC. They found a pronounced 24-h periodicity in the depth gradient of both fluorescence and water temperature during the spring bloom. The diurnal decline in chlorophyll concentrations near the surface was accompanied by an increase in chlorophyll concentrations at greater depth. They attributed this periodicity to diurnal variation in convective mixing, with net sedimentation of phytoplankton during thermal micro-stratification at daytime and net resuspension due to surface cooling at night. Van Haren et al. (1998) estimated the sinking rate of the diatoms in the spring bloom at 50–200 m d^{-1}, which is in the same order of magnitude as earlier estimated sinking rates of 70 m d^{-1} by Passow (1991). In addition, diurnal vertical migration of motile phytoplankton and non-photochemical quenching of chlorophyll fluorescence at high levels of solar irradiance may play a role in the 24-h periodicity. At sites where tidal mixing is too strong for micro-stratification to develop, such as WARP, non-photochemical quenching is probably the dominant process driving 24-h periodicity of chlorophyll fluorescence (Blauw et al., 2012).

In the daily time series, cross correlations with surface PAR showed a negative peak at a time lag of -1 day at all stations except WARP (Fig. 9C1-4). This indicates that chlorophyll concentrations decrease after days with high irradiance. If chlorophyll levels would decrease due to enhanced sinking of phytoplankton on sunny days one would expect to see a negative peak without time lag. A possible explanation for the one day time lag might be that cells have been damaged by photo-inhibition or have down-regulated their pigment content after a day of high-light stress (Anning et al., 2000).

3.3.4. Temperature

In the hourly time series, cross correlations of chlorophyll with air and sea surface temperature showed similar patterns as the cross correlations with PAR, but with a time delay of +2 h for air temperature (Fig. 8D1-4) and a time delay of +5 h for sea surface temperature (Fig. 8E1-4). Since chlorophyll fluorescence reached its minimum at noon, these time delays may not have a causal relationship with chlorophyll but merely indicate that air temperature was highest at on average ~2 h after noon, while sea surface temperature reached its maximum a few hours later in the afternoon.

In the daily time series, cross correlations with sea surface temperature at station WARP showed a 15-day periodicity with negative peaks at a time delay of +2 days (Fig. 9E1). The chlorophyll concentration at this station reached its maximum during spring tide (Fig. 9A1). Hence, the time delay of +2 days of chlorophyll with sea surface temperature may indicate that horizontal mixing of the cross-shore temperature gradient by spring tides is a slower process than the vertical mixing of chlorophyll and SPM profiles. This results in a maximum influence of cold offshore waters 2 days after spring tide. At OYST, the cross correlation with sea surface temperature did not have a distinct periodicity, but did show a significant negative correlation at zero time delay (Fig. 9E4). This indicates that low sea surface temperatures were associated with enhanced surface chlorophyll concentrations, probably because the relatively cold water layers of the deep chlorophyll maximum were mixed to the surface during episodic events with enhanced vertical mixing (Van Haren et al., 1998; Weston et al., 2005). Enhanced surface chlorophyll concentrations induced by mixing events in stratified systems have also been observed by other authors (Jiang et al., 2007; Dickey et al., 2001; Andersen and Prieur, 2000). However, in these studies the increase in chlorophyll concentrations was attributed to enhanced growth due to nutrients being mixed into the surface layer. In that case we would expect to see a time lag of several days between the decrease of sea surface temperature and the increase of chlorophyll concentrations, because phytoplankton growth takes time. In our study, the absence of a time lag suggests that mixing of phytoplankton cells into the surface layer is the dominant process explaining the negative correlation between sea surface temperature and the chlorophyll concentration in the daily time series.

3.3.5. Salinity

In the hourly time series, cross correlations of chlorophyll with salinity show a 12-h 25-min periodicity at WARP and WGAB (Fig. 8F1, F2). This periodicity reflects horizontal transport of water masses of different salinity by the semidiurnal tidal cycle (Blauw et al., 2012), consistent with the peaks at 12 h 25 min in the global wavelet spectra in Fig. 7A and C. The positive cross correlation at zero time lag at WGAB indicates that the more saline water had a higher chlorophyll concentration. At NW10 cross correlations also peaked at lag zero, but there was no periodicity (Fig. 8F3), indicating that the correlation between salinity and chlorophyll fluctuations at NW10 could not be explained by horizontal transport by tidal currents.

In the daily time series, WARP showed a positive cross correlation

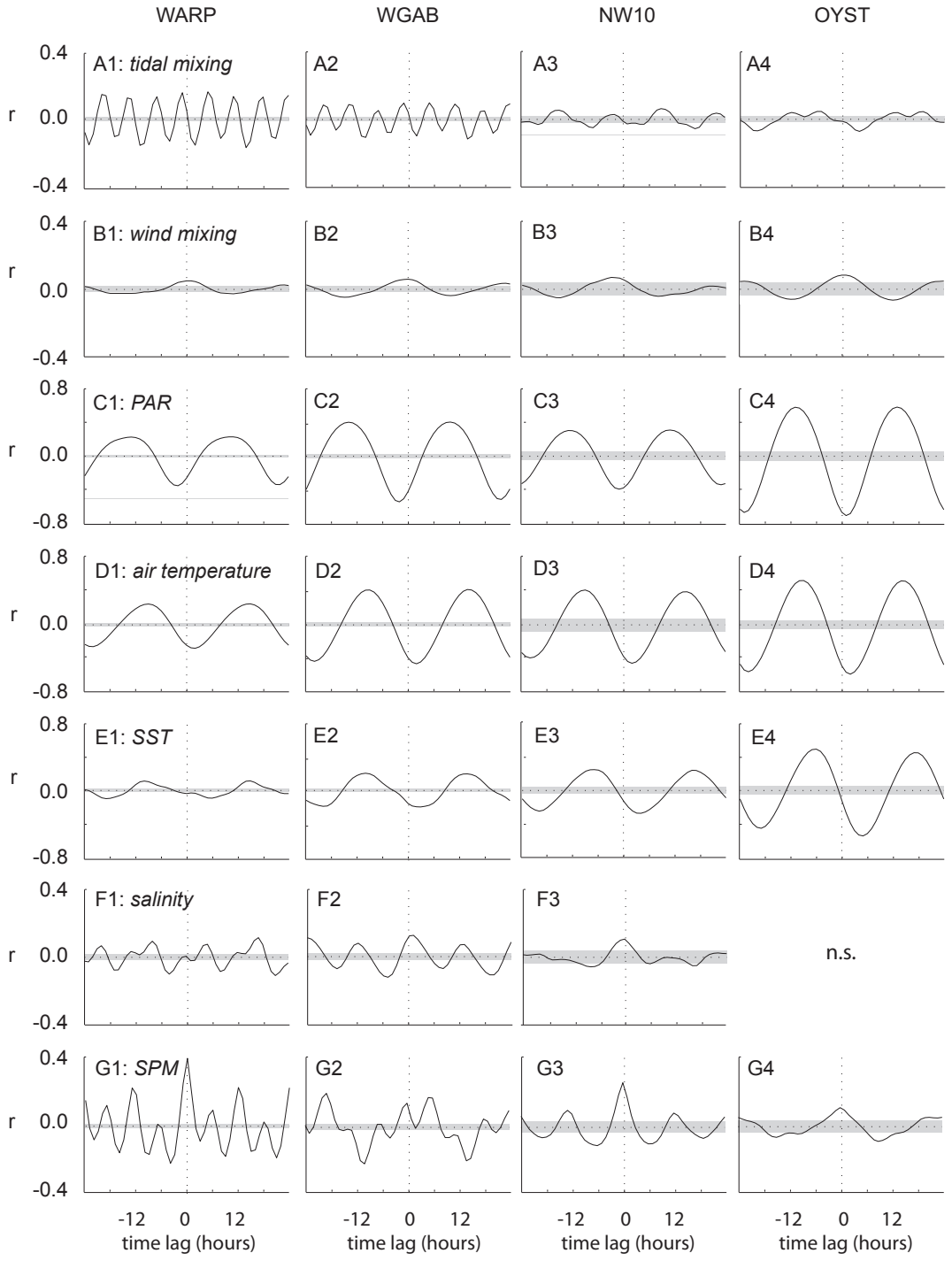

Fig. 8. Cross correlations of hourly chlorophyll data with environmental variables. Cross correlations of hourly time series of chlorophyll with (A) tidal mixing, (B) wind mixing, (C) PAR, (D) air temperature, (E) sea surface temperature (SST), (F) salinity, and (G) SPM. Columns indicate the mooring stations: (1) WARP, (2) WGAB, (3) NW10 and (4) OYST. Peaks exceeding the 95% confidence interval of cross correlation coefficients generated by red noise (horizontal grey band) are significant. Cross correlations that were not significant (n.s.) are omitted.

with salinity at a 15-day periodicity and a lag of + 2 days (Fig. 9F1). Changes in salinity are mostly affected by changes in horizontal mixing, since the vertical profile of salinity at this station is generally uniform (see Blauw et al., 2012). Therefore, the delay between chlorophyll peaks at spring tide and salinity peaks two days after spring tide indicates that mixing of the horizontal cross-shore salinity gradient is slower than mixing of the vertical chlorophyll gradient, as we also observed in the cross correlations with sea surface temperature (Fig. 9E1).

NW10 showed a positive cross correlation of chlorophyll with salinity at zero time lag. This station is located in the Region of Freshwater Influence (ROFI) of the river Rhine along the Dutch coast, characterized by intermittent salinity stratification (Simpson et al., 1993; De Ruijter et al., 1997). The positive correlation indicates that chlorophyll concentrations were higher in offshore waters with high salinity than in low-salinity waters of the river plume, although the latter have higher nutrients concentrations. A possible explanation is that under temporary salinity stratification, phytoplankton cells sink from relatively fresh surface waters of low density to deeper waters with higher salinity and hence higher density. When the salinity

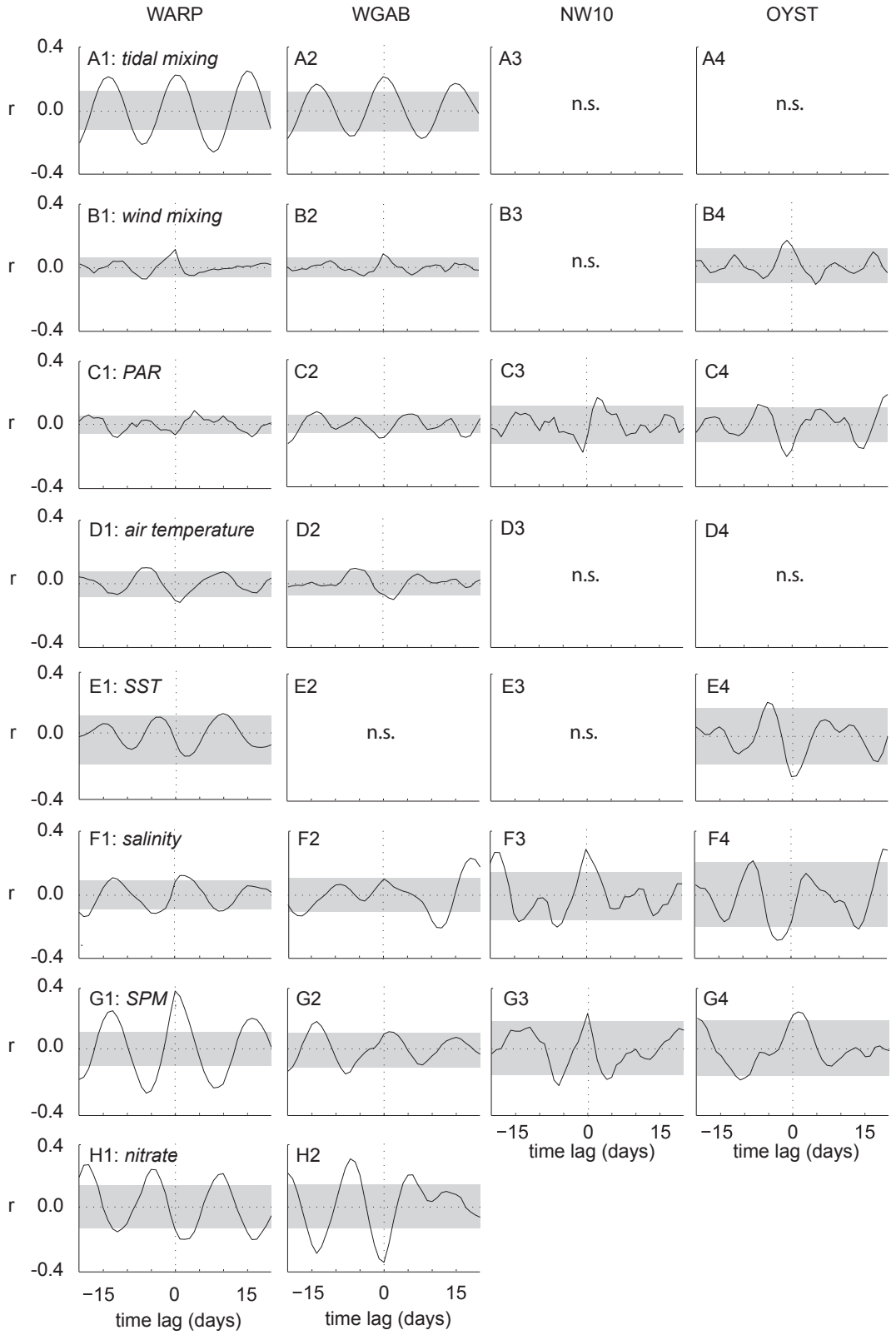

Fig. 9. Cross correlations of daily chlorophyll data with environmental variables. Cross correlations of daily time series of chlorophyll with (A) tidal mixing, (B) wind mixing, (C) PAR, (D) air temperature, (E) sea surface temperature (SST), (F) salinity, (G) SPM, and (H) nitrate. Columns indicate the mooring stations: (1) WARP, (2) WGAB, (3) NW10 and (4) OYST. Peaks exceeding the 95% confidence interval of cross correlation coefficients generated by red noise (horizontal grey band) are significant. Cross correlations that were not significant (n.s.) are omitted.

stratification breaks down, the higher phytoplankton concentrations in the deeper layers are mixed back to the surface. This process has been observed and described near station NW10 by Joordens et al. (2001) and McCandliss et al. (2002).

3.3.6. SPM

Cross correlations with (log-transformed) SPM in the hourly time series showed a positive peak at lag zero at all stations (Fig. 8G1-4). This indicates that chlorophyll fluctuates in phase with SPM. The periodicity of the cross correlations differed between the stations, with a combination of 6-h and 12-h periodicity at WARP, 6-, 12- and 24-h periodicity at WGAB, 12-h periodicity at NW10 and 24-h periodicity at OYST, consistent with the periodicities of the chlorophyll fluctuations identified by the global wavelet spectra (Fig. 7A, C, E, and G).

In the daily time series, cross correlations of chlorophyll with SPM showed a positive peak with an approximately zero time lag at all stations (Fig. 9G1-4), indicating that chlorophyll fluctuated in phase with SPM at the daily time scale as well. At WARP and WGAB the cross correlations with SPM showed 15-day periodicity (Fig. 9G1-2), consistent with the 15-day periodicity of the chlorophyll fluctuations at these stations (Fig. 7B and D).

3.3.7. Nitrate

Sufficient nitrate data for cross correlation analysis were only available for the daily time series of stations WARP and WGAB. Both stations showed cross correlations between chlorophyll and nitrate at a 15-day periodicity, with a negative peak at lag +2 days for WARP and at lag zero for WGAB (Fig. 9H1 and H2). The 15-day periodicity and time lag of +2 days at WARP was also observed in the cross correlations with sea surface temperature (Fig. 9E1) and salinity (Fig. 9F1). They reflect the effect of horizontal mixing by the spring-neap tidal cycle on cross-shore concentration gradients, with maximum influence of offshore waters two days after spring tide.

3.4. Generalized additive models

Figs. 10–12 show the smooth functions of the explanatory variables that were significant in the GAM models of the hourly, daily and biweekly time series, respectively. Confidence intervals are shown for each subset of the time series for which the explanatory variable was significant. Variables with little explanatory power have almost horizontal smooth curves, while variables with most explanatory power show steep smooth curves, covering a relatively large range along the y-axis.

For the hourly time series, the GAM models explained 25–51% of the variation in the chlorophyll concentrations (Table 2). At all four stations chlorophyll fluorescence was negatively affected by PAR (Fig. 10A). This was also observed in the cross correlations, and can be explained by non-photochemical quenching of chlorophyll fluorescence (Kiefer, 1973; Blauw et al., 2012) and/or by enhanced micro-stratification (van Haren et al., 1998) at high PAR levels. At WARP, the chlorophyll concentration showed a strong positive relation with SPM (Fig. 10D1), consistent with the positive cross correlation between chlorophyll and SPM fluctuations at this station (Fig. 8G1). At NW10, the chlorophyll concentration showed a distinct positive relationship with both SPM and salinity (Fig. 10D3 and E3).

For the daily time series, the GAM models explained only 13 to 22% of the observed variation (Table 2). At WARP, SPM was the dominant explanatory variable and salinity the only other significant variable (Fig. 11A1 and B1). Apparently, effects of tidal range and wind speed, that were significant in the cross correlations (Fig. 9A1 and B1), were subsumed in the SPM fluctuations and had no significant additional explanatory power. At WGAB the opposite was observed: tidal range and wind speed had a significant positive effect on the chlorophyll concentration (Fig. 11C2 and D2) while the additional effect of SPM was insignificant. Nitrate had a significant negative effect on chlorophyll concentrations at WGAB, consistent with the cross correlations. At NW10, the chlorophyll concentration showed a strong positive relation with both SPM and salinity (Fig. 11A3 and B3). At OYST, the chlorophyll concentration was negatively related to both sea surface temperature and PAR (Fig. 11A4 and D4), consistent with the cross correlations (Fig. 9C4 and E4).

For the biweekly time series, the GAM models explained 27–63% of the variation in the rates of change of the chlorophyll concentration (Table 2). At WARP, SPM had again the largest explanatory power, with a positive rate of change of the chlorophyll concentration at SPM $> 10\,g\,m^{-3}$ and a negative rate of change at lower SPM concentrations (Fig. 12F1). This pattern reflects the gradual increase in chlorophyll concentrations when SPM concentrations were relatively high in late winter and early spring, and the decline of the spring bloom when SPM concentrations were lower in early summer (Fig. 3B). Tidal range had a significant effect at WARP (Fig. 12D1), even though both the semi-diurnal and spring-neap variability were filtered out by the 15-day averaging of the biweekly time series. The remaining variability in the biweekly time series of tidal range at WARP was dominated by the 28-day periodicity of the apogee- perigee cycle (Blauw et al., 2012), which is a less conspicuous component of the tidal motions but apparently still powerful enough to affect the chlorophyll concentrations. Nitrate showed clear seasonal variation at WARP, with low nitrate concentrations in summer (Fig. 3C). However, summer nitrate concentrations were less depleted at WARP than at WGAB and OYST (Table 1), and nitrate was not identified as a significant variable at WARP by the GAM model (Fig. 12), suggesting that nitrogen was not a major limiting factor at this station. Since we lacked data on other nutrients, it is difficult to establish which factor did limit phytoplankton growth at WARP. However, according to a field study by Weston et al. (2008), summer populations of large diatoms at WARP were limited by low light and silicate availability while small flagellates were controlled by zooplankton grazing.

At the other three stations the rate of change of chlorophyll showed a strong positive relationship with the nitrate concentration, with high growth rates in spring and lower growth rates in summer (Fig. 12B2–B4). Additionally, at NW10 changes in salinity had a strong impact on chlorophyll fluctuations (Fig. 12C3). This suggests that physical mixing and transport processes in the river plume of the Rhine also affect chlorophyll dynamics at the time scale of weeks to months. At OYST, PAR showed a strong positive effect on chlorophyll growth rates (Fig. 12A4). The negative relation with the rate of change in sea surface temperature (Fig. 12E4) indicates that the seasonal rise in sea surface temperature coincided with a gradual decline of the chlorophyll concentration after the spring bloom (in April - July; Fig. 6B and D).

3.5. Predictability of chlorophyll fluctuations

To assess the overall predictability of the chlorophyll concentrations from the environmental variables, we used the GAM models obtained at the three time scales to reconstruct the chlorophyll time series. Subsequently, we calculated R^2 values between the chlorophyll concentrations predicted by the GAM models and the observed hourly chlorophyll time series. For comparison, we also calculated R^2 values between a null model that predicts the chlorophyll concentration based on autocorrelation only and the observed chlorophyll time series.

Fluctuations in R^2 values of the null model (Fig. 13) reflect fluctuations in chlorophyll fluorescence within the day, which are particularly strong at WGAB and OYST. The R^2 value of the null model dropped below 0.5 within 5 days at all four stations, indicating that measurements of the chlorophyll concentration remain reasonable estimates of the chlorophyll concentration for only a few consecutive days, whereas measurements of two weeks ago are no longer representative of the actual chlorophyll concentration. In contrast, the R^2 values of the GAM models remained above 0.5 for 2 to 4 weeks (Fig. 13). This shows that the environmental variables included in the

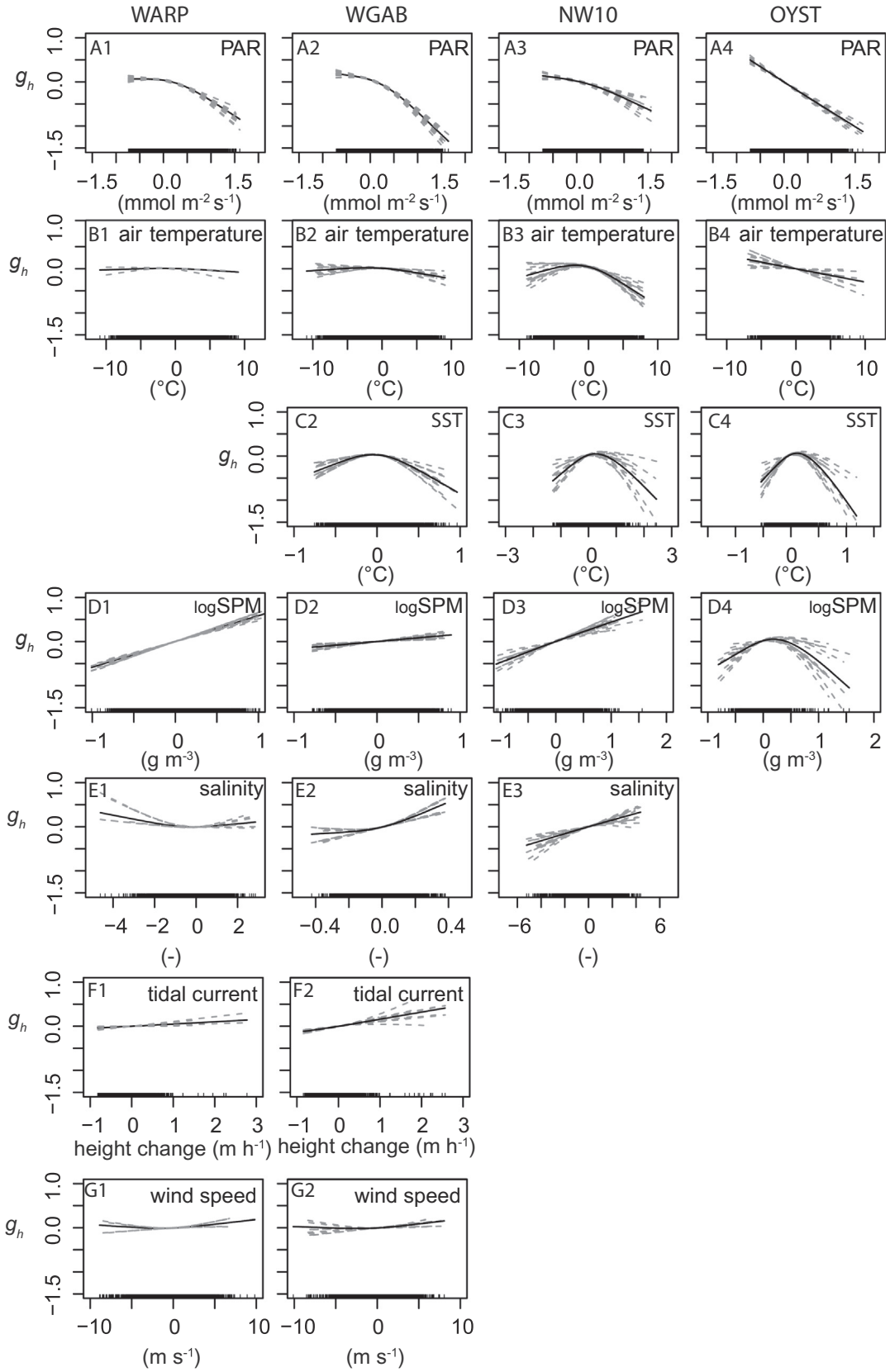

Fig. 10. GAM models of hourly chlorophyll data. The smooth functions g_h (solid lines) describe the effects of environmental variables on the chlorophyll concentrations in the hourly time series. They are based on GAM models fitted to the entire hourly time series. The 95% confidence intervals (dashed lines) of the smooth functions are shown for each subset of the time series for which the environmental variable was significant. Smooth functions that were not significant in any of the subsets were omitted from the GAM models. Tick marks on the x-axis indicate the distribution of the data points. Columns indicate the mooring stations: (1) WARP, (2) WGAB, (3) NW10 and (4) OYST.

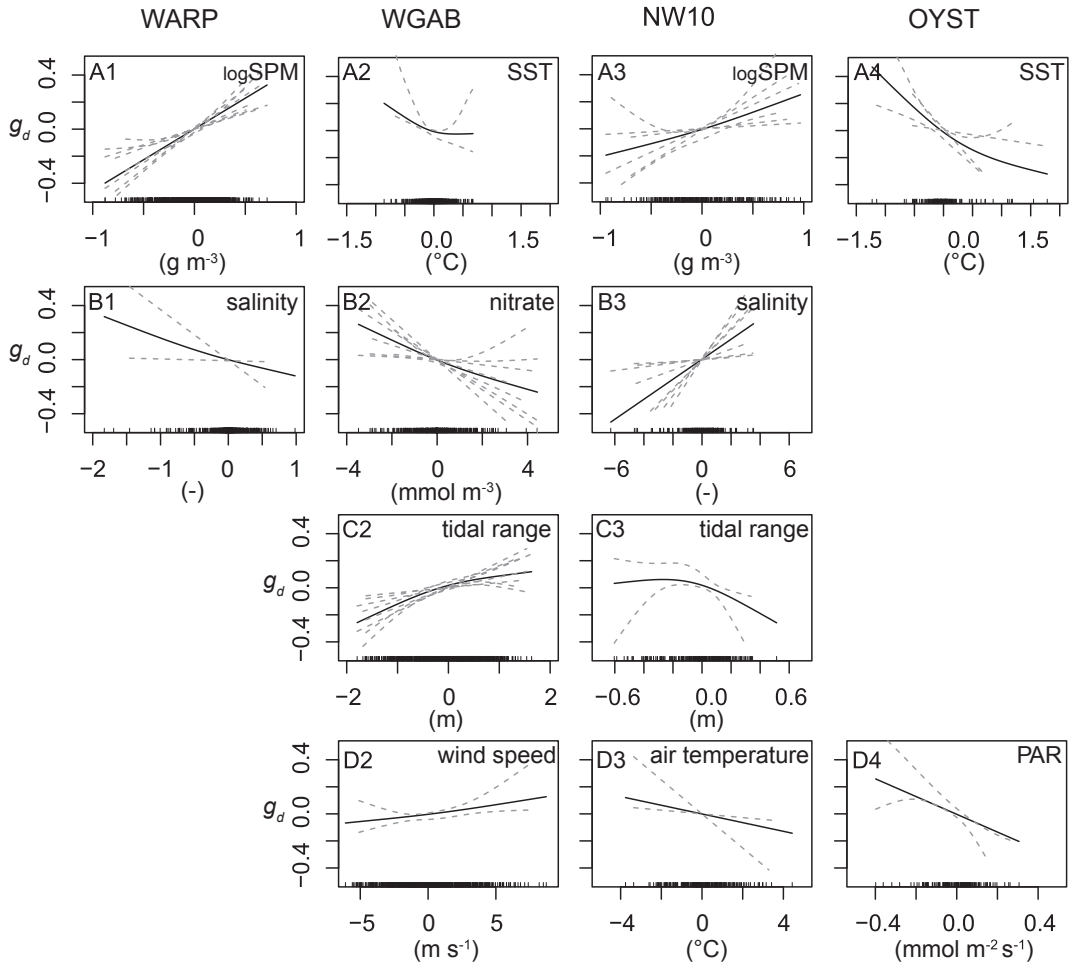

Fig. 11. GAM models of daily chlorophyll data. The smooth functions g_d (solid lines) describe the effects of environmental variables on the chlorophyll concentrations in the daily time series. They are based on GAM models fitted to the entire daily time series. The 95% confidence intervals (dashed lines) of the smooth functions are shown for each subset of the time series for which the environmental variable was significant. Smooth functions that were not significant in any of the subsets were omitted from the GAM models. Tick marks on the x-axis indicate the distribution of the data points. Columns indicate the mooring stations: (1) WARP, (2) WGAB, (3) NW10 and (4) OYST.

GAM models strongly improved the predictability and explained a large fraction of the variation in chlorophyll concentration.

3.6. Limitations of the monitoring approach

Part of the chlorophyll fluctuations in our study can be attributed to the applied measurement techniques. Due to non-photochemical quenching, the chlorophyll fluorescence signal may underestimate the actual chlorophyll concentrations during daytime, which leads to diurnal variation in chlorophyll fluorescence. This effect was particularly strong in the clear waters of OYST and WGAB. Dark-adaptation of phytoplankton for several minutes prior to the fluorescence measurement could help to overcome this problem. Alternatively, only nighttime measurements can be used, as we did in the daily time series, but then information on short-term chlorophyll fluctuations during daytime will of course be lacking.

Vertical redistribution of phytoplankton populations by the interplay of particle sinking and mixing is a major source of variability in the phytoplankton concentrations of coastal waters. Hence, surface measurements may underestimate the total phytoplankton biomass, if the phytoplankton population has not changed but has been mixed deeper in the water column. The sub-surface chlorophyll maximum in stratified areas due to in-situ growth is another reason why surface measurements are often not representative of total phytoplankton biomass over depth. Many monitoring programs, including monitoring by remote sensing, focus on surface observations. Therefore caution is required when interpreting such data, because part of the population might have been overlooked. Depth-integrated sampling might reduce this problem.

Horizontal redistribution is also a major source of phytoplankton variability observed in our study. This is illustrated by the 12-h periodicity and significant cross correlations with salinity. A better representation of this spatial variability will require other monitoring methods such as satellite remote sensing or transect measurements, complementary to time series at fixed locations. However, as illustrated by our results, at least part of the horizontal variability is driven by the semidiurnal tidal cycle, and monitoring this variation will therefore need a high temporal resolution of these spatial monitoring techniques.

Finally, an important issue in many monitoring approaches is that several environmental variables (e.g., temperature, irradiance) tend to co-vary on a seasonal time scale, which may confound statistical analyses. In our study, we detrended the hourly and daily time series of the chlorophyll fluctuations and environmental variables to remove the seasonal component. The seasonal component was still present in the biweekly time series, although differencing of the chlorophyll fluorescence suppressed the seasonality in the chlorophyll signal to some extent and the seasonal cycle was not the same for all variables at all stations. For example, the annual maximum of water temperature occurred months later than the annual maximum of solar irradiance, the annual minimum in nitrate concentrations was often earlier than the annual maximum in irradiance, and salinity showed more variability at station NW10 than at the other stations. Therefore, seasonal co-variation of different variables may have confounded our analysis of the

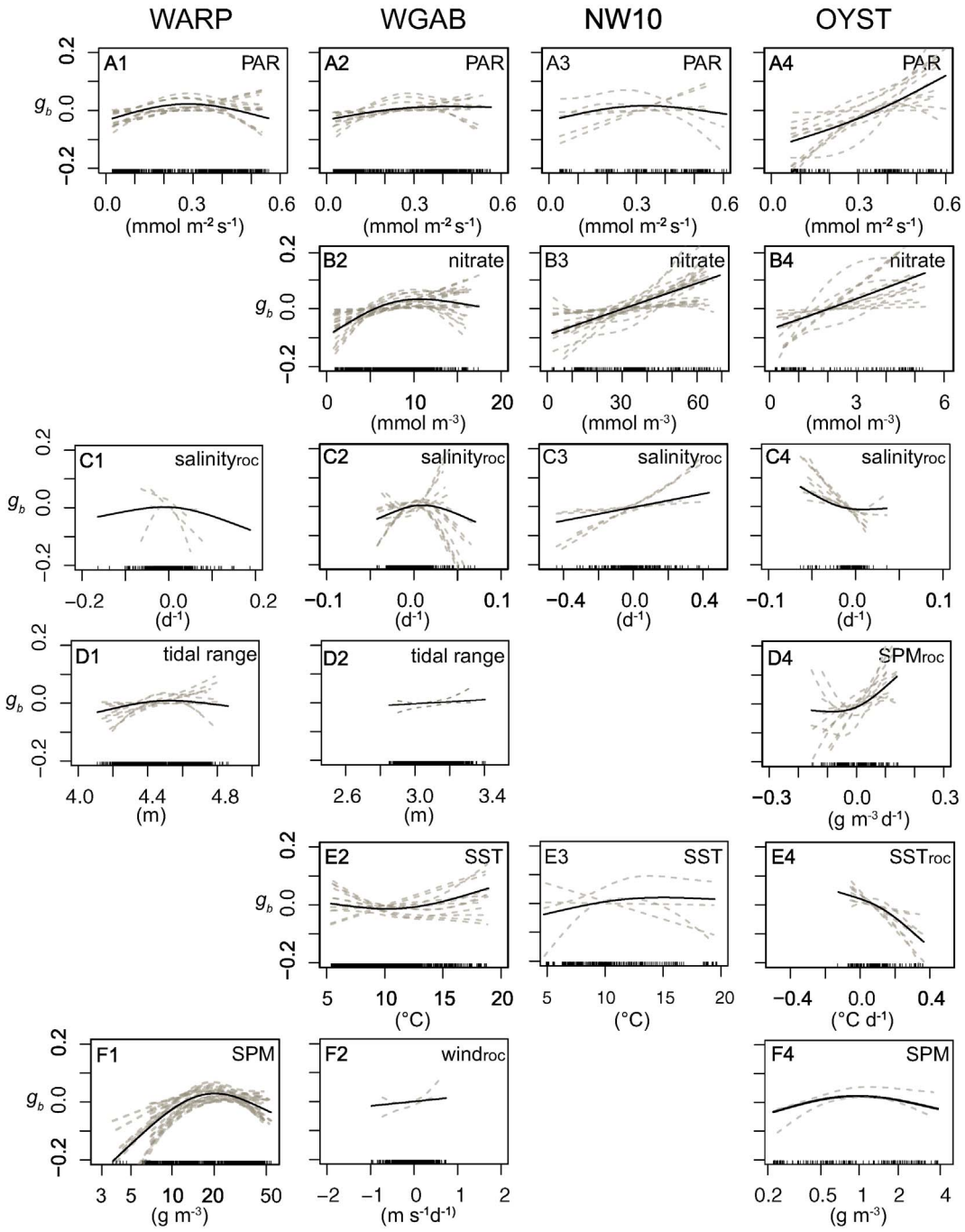

Fig. 12. GAM models of biweekly chlorophyll data. The smooth functions g_b (solid lines) describe the effects of environmental variables on the chlorophyll concentrations in the biweekly time series. They are based on GAM models fitted to the entire biweekly time series. The 95% confidence intervals (dashed lines) of the smooth functions are shown for each subset of the time series for which the environmental variable was significant. Smooth functions that were not significant in any of the subsets were omitted from the GAM models. Tick marks on the x-axis indicate the distribution of the data points. Columns indicate the mooring stations: (1) WARP, (2) WGAB, (3) NW10 and (4) OYST. The addition 'roc' to an environmental variable indicates that the graph is based on the rate of change of the environmental variable.

biweekly time series, although we could still discriminate between the effects of different environmental variables to some extent.

3.7. Advantages of long-term high-resolution monitoring

Our results show that high-resolution monitoring can reveal striking phytoplankton fluctuations at hourly to daily time scales. The magnitude of these short-term fluctuations can be 25–75% of the seasonal variation. This variability should not be dismissed as "random noise", but is a key feature of phytoplankton dynamics in coastal waters affected by wind and tides.

Studies of short-term fluctuations are often based on short time series of one or several days (Brunet and Lizon, 2003), one bloom event (van Haren et al., 1998) or one spring-neap cycle (Joordens et al., 2001). Although these studies may all provide interesting information, they cannot tell whether their observations are representative of the situation in other times of the year. In contrast, long-term high-resolution time series provide detailed insight in the long-term consistency of the phytoplankton fluctuations across different time scales and thereby reduce the risk of spurious correlations.

Another key advantage of high-resolution monitoring is that the chlorophyll fluctuations can be linked to fluctuations of other

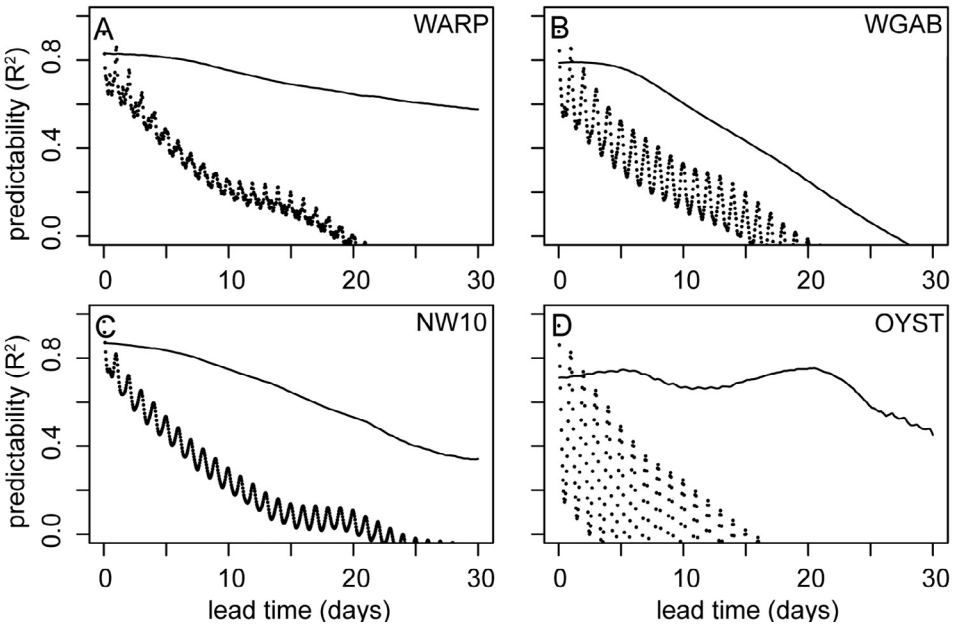

Fig. 13. Predictability of chlorophyll concentrations. Predictability (expressed as R^2 values) of the hourly chlorophyll concentration at lead times of 1 to 30 days ahead. The predictions are shown for a null model based on autocorrelation only (dotted lines) and for a full model including all environmental variables that were significant in the GAM models (solid lines). (A) WARP. (B) WGAB. (C) NW10. (D) OYST.

environmental variables, which enables a detailed analysis of the potential environmental drivers. At station WARP, for example, SPM and tidal range had a zero time lag with the chlorophyll fluctuations, whereas sea surface temperature, salinity and nitrate all had a time lag of +2 days. This suggests that fluctuations of chlorophyll, SPM and tidal range were driven by the same process (vertical mixing), whereas fluctuations of sea surface temperature, salinity and nitrate were driven by another process (horizontal mixing). The positive time lag of sea surface temperature, salinity and nitrate further suggests that changes in sea surface temperature, salinity and nitrate were not the cause of the chlorophyll fluctuations, but rather that sea surface temperature, salinity and nitrate followed changes in chlorophyll, SPM and tidal range with some delay (e.g., due to horizontal mixing of different water masses, with a maximum influence of cold, saline and nitrate-poor offshore waters 2 days after spring tide). In low-resolution time series this subtle time delay would not have been visible, which may easily have led to erroneous conclusions.

Many marine monitoring programs sample phytoplankton at a monthly frequency. Our results demonstrate that this is clearly not enough to capture the variability of phytoplankton populations in coastal waters. In our time series chlorophyll measurements were a reasonable estimate of chlorophyll concentrations up to 5 days ahead, but lost their reliability at longer time scales (Fig. 13). This suggests that a minimum measurement interval of 5 days is required to describe the actual chlorophyll concentrations, assuming that the sampling time is tuned to the tidal cycle. Moreover, if the goal is not only a description but also an understanding of the underlying processes, then a higher sampling frequency will be essential. Our results show that phytoplankton concentrations in coastal environments respond strongly to tidal mixing and weather variability at hourly to weekly time scales. Hence, an understanding of the phytoplankton variability in coastal waters and their response to environmental change will require sampling at these relevant time scales.

3.8. Implications for food web dynamics

Phytoplankton is a major food source for zooplankton and benthic organisms such as filter-feeding bivalves. Phytoplankton fluctuations are therefore likely to affect food web dynamics. Although effects of seasonality on aquatic food webs have been investigated by various studies (e.g., Dakos et al., 2009; Koeller et al., 2009; McMeans et al., 2015), effects of environmental variability at shorter time scales on food web dynamics have received less attention. Experimental studies have shown that fluctuations in zooplankton abundances are strongly coupled to phytoplankton fluctuations, and may show predator-prey oscillations with typical periodicities of a few weeks (Fussmann et al., 2000; Benincà et al., 2009). Microzooplankton has short generation times of only a few days. Microzooplankton abundances might therefore be able to track phytoplankton fluctuations generated by the spring-neap tidal cycle, and it is conceivable that forcing by phytoplankton fluctuations may affect the magnitude of the zooplankton fluctuations. For organisms with longer life spans, such as benthic filter feeders, phytoplankton fluctuations at seasonal and inter-annual time scales are in general more likely to affect abundance. For these organisms day-to-day phytoplankton fluctuations will affect individual growth rates rather than population abundances. However, larval survival in spring may be strongly affected by biweekly fluctuations in phytoplankton concentrations. This suggests that the timing of spawning in relation to the spring-neap tidal cycle may have an impact on the abundance of filter-feeding bivalves later in the year.

4. Conclusions

4.1. Regional differences in dominant drivers

Our results confirm that the processes driving chlorophyll fluctuations differ in different regions of the North Sea. At the macro-tidal stations (WARP and WGAB), chlorophyll fluctuations were strongly affected by the tidal cycle. We found clear tidal signatures of both the semi-diurnal cycle (periodicities of 6 h 12 min and 12 h 25 min) and the spring-neap cycle (15 days).

At the shallow coastal stations (WARP and NW10) the chlorophyll fluctuations showed a strong positive relation with SPM concentrations at the hourly and daily time scale. These results indicate that sinking and mixing processes played a dominant role, possibly in the form of single cells but resuspension of cell aggregates associated with benthic fluff may also play a role (Joordens et al., 2001). In the region of freshwater influence (ROFI) along the Dutch coast, the chlorophyll fluctuations were also associated with salinity variations at all investigated time scales (NW10). At hourly to daily time scales this is presumably due to tidal and wind-induced transport of water masses with different salinities and chlorophyll concentrations. At time scales of weeks, variation in river discharge of the Rhine and the spatial extent of the river plume may play a role.

In relatively deep and clear waters further offshore (WGAB and OYST), we found signatures of diurnal non-photochemical quenching (Kiefer, 1973; Blauw et al., 2012) and micro-stratification (van Haren et al., 1998). Moreover, these stations showed a positive relation of the chlorophyll concentration with wind speed and negative relation with sea surface temperature in the daily time series, indicative of entrainment of cold water with associated phytoplankton from deeper layers during days with high wind speeds. During summer, nitrate concentrations were more strongly depleted at these deep offshore stations than at the shallow coastal stations (Table 1). Particularly in the central North Sea (OYST), seasonal stratification played a major role, resulting in nutrient-depleted surface waters with a gradually decreasing chlorophyll concentrations in the surface layer during summer.

4.2. Dominant drivers across time scales

Our analysis shows that the major environmental drivers of phytoplankton variability are different at different time scales:

1. Hour-to-hour variability of the phytoplankton concentration was mainly driven by variation in sinking and vertical mixing rates generated by tidal currents and wind action and by horizontal displacement of water masses by the semi-diurnal tidal cycle. The importance of tidal mixing is clearly illustrated by the 6-h 12-min periodicity of chlorophyll fluctuations in phase with SPM fluctuations at the macro-tidal stations. The importance of horizontal displacement is illustrated by the 12-h 25-min periodicity of chlorophyll fluctuations in phase with salinity fluctuations. Furthermore, chlorophyll fluorescence was strongly affected by the day-night cycle of solar irradiance. Non-photochemical quenching of the fluorescence signal at high light intensities is likely to play a role in this 24-h periodicity.
2. Day-to-day variability was predominantly driven by variation in sinking and mixing processes generated by the spring-neap tidal cycle and by wind action. The role of the spring-neap cycle is illustrated by the observed 15-day periodicity. Cross-correlations with environmental variables indicative of vertical mixing (such as SPM) suggest that sinking and mixing processes were key drivers of the day-to-day variability of chlorophyll concentrations.
3. At the time scale of weeks to months, variation in nutrient and light conditions were the dominant drivers of changes in phytoplankton concentrations. These results correspond with other studies using GAM models, which also identified nutrients, light and temperature as the main drivers of seasonal phytoplankton variability (Stenseth et al., 2006; Llope et al., 2009). Additionally, physical processes still play a role at this time scale, as illustrated by the significance of tidal mixing, salinity and temperature in GAM models of the bi-weekly time series.

Hence, in line with previous studies (Brunet and Lizon, 2003; Llope et al., 2009), physical transport processes dominated phytoplankton variability at short time scales (hour-to-hour), whereas biological growth and loss processes were more important at time scales of weeks to months. The predictability of phytoplankton variability was highest at the time scale of weeks to months in the central North Sea ($R^2 = 0.63$), and lowest at the daily time scale at macro-tidal stations WARP ($R^2 = 0.15$) and WGAB ($R^2 = 0.13$) (Table 2). This pattern reflects the highly dynamic nature of the macro-tidal systems versus the more stable and seasonally stratified conditions in the central North Sea.

Plankton are often hypothesized to behave like passive tracers at short time scales (Harris, 1980; Denman and Gargett, 1995). However, our results show that phytoplankton fluctuations deviated from the fluctuations of passive tracers like salinity and temperature. Variation in sinking and mixing processes generated by wind and tides explained much of the hour-to-hour and day-to-day chlorophyll fluctuations. In particular, at the macro-tidal stations, phytoplankton and SPM showed fluctuations with a 6 h 12 min and 12 h 25 min periodicity, whereas salinity and temperature fluctuated only at a 12 h 25 min periodicity (Blauw et al., 2012). Moreover, at these time scales, phytoplankton fluctuated in phase with SPM. Hence, at time scales of hours to days, phytoplankton behaved as particles rather than passive tracers.

Acknowledgements

This publication is dedicated to the memory of our colleague and co-author professor Remi Laane, a warm advocate of marine monitoring programs. We thank Cefas (United Kingdom) for the mooring data (collected under Defra-funded contracts AE004, SLA25, C1041), and the British Oceanographic Data Centre and Rijkswaterstaat for the tidal data. We thank the Royal Dutch Meteorological Institute (KNMI) for the meteorological observations. We thank F. Zijl, R. E. Uittenbogaard, G. J. de Boer and M. Blaas for fruitful discussions and information on tides and mixing processes, and three anonymous reviewers for their helpful comments on the manuscript. This research was supported by the ZKO project "Integrated monitoring of carrying capacity in coastal waters" funded by the Netherlands Organisation of Scientific Research (NWO), and by the Strategic Research program of Deltares.

Appendix A. Supplementary material

Supplementary data associated with this article can be found, in the online version, at http://dx.doi.org/10.1016/j.pocean.2018.01.005.

References

Andersen, V., Prieur, L., 2000. One-month study in the open NW Mediterranean Sea (DYNAPROC experiment, May 1995): overview of the hydrobiogeochemical structures and effects of wind events. Deep-Sea Res. I 47, 397–422.
Anning, T., Maclntyre, H.L., Pratt, S.M., Sammes, P.J., Gibb, S., Geider, R.J., 2000. Photoacclimation in the marine diatom *Skeletonema costatum*. Limnol. Oceanogr. 45, 1807–1817.
Benincà, E., Jöhnk, K.D., Heerkloss, R., Huisman, J., 2009. Coupled predator–prey oscillations in a chaotic food web. Ecol. Lett. 12, 1367–1378.
Belgrano, A., Lindahl, O., Hernroth, B., 1999. North Atlantic Oscillation primary productivity and toxic phytoplankton in the Gullmar Fjord, Sweden (1985–1996). Proc. Roy. Soc. London B: Biol. Sci. 266, 425–430.
Blauw, A.N., Benincà, E., Laane, R.W.P.M., Greenwood, N., Huisman, J., 2012. Dancing with the tides: fluctuations of coastal phytoplankton orchestrated by different oscillatory modes of the tidal cycle. PLoS ONE 7 (11), e49319. http://dx.doi.org/10.1371/journal.pone.0049319.
Breton, E., Rousseau, V., Parent, J.Y., Ozer, J., Lancelot, C., 1996. Hydroclimatic modulation of diatom/*Phaeocystis* blooms in nutrient-enriched Belgian coastal waters (North Sea). Limnol. Oceanogr. 51, 1401–1409.
Brunet, C., Lizon, F., 2003. Tidal and diel periodicities of size-fractionated phytoplankton pigment signatures at an offshore station in the southeastern English Channel. Estuarine Coastal Shelf Sci. 56, 833–843. http://dx.doi.org/10.1016/s0272-7714(02)00323-2.
Cazelles, B., Chavez, M., Berteaux, D., Ménard, F., Vik, J.O., et al., 2008. Wavelet analysis of ecological time series. Oecologia 156, 287–304. http://dx.doi.org/10.1007/s00442-008-0993-2.
Cloern, J.E., Jassby, A., 2010. Patterns and scales of phytoplankton variability in estuarine–coastal ecosystems. Estuaries Coasts 33, 230–241. http://dx.doi.org/10.1007/s12237-009-9195-3.
Dakos, V., Benincà, E., van Nes, E.H., Philippart, C.J., Scheffer, M., Huisman, J., 2009. Interannual variability in species composition explained as seasonally entrained chaos. Proc. Roy. Soc. London B: Biol. Sci. 276, 2871–2880.
De Boer, G.J., Pietrzak, J.D., Winterwerp, J.C., 2009. SST observations of upwelling induced by tidal straining in the Rhine ROFI. Cont. Shelf Res. 29, 263–277.
Denman, K.J., Gargett, A.E., 1995. Biological-physical interactions in the upper ocean: the role of vertical and small scale transport processes. Annu. Rev. Fluid Mech. 27, 225–256.
De Ruijter, W.P.M., Visser, A.W., Bos, W.G., 1997. The Rhine outflow: a prototypical pulsed discharge plume in a high energy shallow sea. J. Mar. Syst. 12, 263–276.
Dickey, T., Zedler, S., Yu, X., Doney, S.C., Frye, D., et al., 2001. Physical and biogeochemical variability from hours to years at the Bermuda Testbed Mooring site: June 1994-March 1998. Deep-Sea Res. II 48, 2105–2140.
Franks, P.J.S., 2005. Plankton patchiness, turbulent transport and spatial spectra. Mar. Ecol. Prog. Ser. 294, 295–309.
Fussmann, G.F., Ellner, S.P., Shertzer, K.W., Hairston Jr, N.G., 2000. Crossing the Hopf bifurcation in a live predator-prey system. Science 290, 1358–1360.
Harris, G.P., 1980. Temporal and spatial scales in phytoplankton ecology: mechanisms,

methods, models, and management. Can. J. Fish. Aquat. Sci. 37, 877–900.
Hastie, T., Tibshirani, R.J., 1990. Generalized Additive Models. Chapman & Hall, London, UK.
Gonzalez, N.E., Muller-Karger, F.E., Estrada, S.C., de los Reyes, R.P., del Rio, I.V., et al., 2000. Near-surface phytoplankton distribution in the western Intra-Americas Sea: the influence of El Nino and weather events. J. Geophys. Res. 105, 14029–14043.
Greenwood, N., Parker, E.R., Fernand, L., Sivyer, D.B., Weston, K., et al., 2010. Detection of low bottom water oxygen concentrations in the North Sea: implications for monitoring and assessment of ecosystem health. Biogeosciences 7, 1357–1373. http://dx.doi.org/10.5194/bg-7-1357-2010.
Grinsted, A., Moore, J.C., Jevrejeva, S., 2004. Application of the cross wavelet transform and wavelet coherence to geophysical time series. Nonlinear Processes Geophys. 11, 561–566.
Jiang, S., Dickey, T.D., Steinberg, D.K., Madin, L.P., 2007. Temporal variability of zooplankton biomass from ADCP backscatter time series data at the Bermuda Testbed Mooring site. Deep-Sea Res. I 54, 608–636. http://dx.doi.org/10.1016/j.dsr.2006.12.011.
Joordens, J.C.A., Souza, A.J., Visser, A., 2001. The influence of tidal straining and wind on suspended matter and phytoplankton distribution in the Rhine outflow region. Cont. Shelf Res. 21, 301–325.
Kiefer, D.A., 1973. Fluorescence properties of natural phytoplankton populations. Mar. Biol. 22, 263–269.
Klein Tank, A.M.G., Wijngaard, J.B., Können, G.P., Böhm, R., Demarée, G., et al., 2002. Daily dataset of 20th-century surface air temperature and precipitation series for the European Climate Assessment. Int. J. Climatol. 22, 1441–1453.
Koeller, P., Fuentes-Yaco, C., Platt, T., Sathyendranath, S., Richards, A., et al., 2009. Basin-scale coherence in phenology of shrimps and phytoplankton in the North Atlantic Ocean. Science 324, 791–793.
Kolmogorov, A.N., 1941. The local structure of turbulence in an incompressible viscous fluid for very large Reynolds number. Comptes Rendus de l'Académie des Sciences USSR 30, 301–305.
Llope, M., Chan, K.S., Ciannelli, L., Reid, P.C., Stige, L.C., Stenseth, N.C., 2009. Effects of environmental conditions on the seasonal distribution of phytoplankton biomass in the North Sea. Limnol. Oceanogr. 54, 512–524. http://dx.doi.org/10.4319/lo.2009.54.2.0512.
Mann, K.H., Lazier, J.R.N., 2009. Dynamics of Marine Ecosystems: Biological-physical Interactions in the Oceans. Blackwell Publishing Ltd, USA.
McCandliss, R.R., Jones, S.E., Hearn, M., Latter, R., Jago, C.F., 2002. Dynamics of suspended particles in coastal waters (southern North Sea) during a spring bloom. J. Sea Res. 47, 285–302. http://dx.doi.org/10.1016/S1385-1101(02)00123-5.
McMeans, B.C., McCann, K.S., Humphries, M., Rooney, N., Fisk, A.T., 2015. Food web structure in temporally-forced ecosystems. Trends Ecol. Evol. 30, 662–672.
McQuatters-Gollop, A., Vermaat, J.E., 2011. Covariance among North Sea ecosystem state indicators during the past 50 years: contrasts between coastal and open waters. J. Sea Res. 65, 284–292. http://dx.doi.org/10.1016/j.seares.2010.12.004.
Mills, D.K., Laane, R.W.P.M., Rees, J.M., Rutgers van der Loeff, M., Suylen, J.M., Pearce, D.J., Sivyer, D.B., Heins, C., Platt, K., Rawlinson, M., 2003. Smartbuoy: a marine environmental monitoring buoy with a difference. Elsevier Oceanogr. Ser. 69, 311–316.
Ottersen, G., Planque, B., Belgrano, A., Post, E., Reid, P.C., Stenseth, N.C., 2001. Ecological effects of the North Atlantic Oscillation. Oecologia 128, 1–14. http://dx.doi.org/10.1007/s004420100655.
Passow, U., 1991. Species-specific sedimentation and sinking velocities of diatoms. Mar. Biol. 108, 449–466.
Richardson, A.J., Schoeman, D.S., 2004. Climate impact on plankton ecosystems in the Northeast Atlantic. Science 305, 1609–1612. http://dx.doi.org/10.1126/science.1100958.
Sharples, J., Ross, O.N., Scott, B.E., Greenstreet, S.P., Fraser, H., 2006. Inter-annual variability in the timing of stratification and the spring bloom in the North-western North Sea. Cont. Shelf Res. 26, 733–751.
Simpson, J.H., Bos, W.G., Schirmer, F., Souza, A.J., Rippeth, T.P., et al., 1993. Periodic stratification in the Rhine ROFI in the North Sea. Oceanol. Acta 16, 23–32.
Sommer, U., Adrian, R., De Senerpont, Domis L, Elser, J.J., Gaedke, U., et al., 2012. Beyond the Plankton Ecology Group (PEG) model: mechanisms driving plankton succession. Annu. Rev. Ecol. Evol. Syst. 43, 429–448. http://dx.doi.org/10.1146/annurev.ecolsys.39.110707.173549.
Stenseth, N.C., Llope, M., Anadón, R., Ciannelli, L., Chan, K., Hjermann, D.Ø., Bagøien, E., Ottersen, G., 2006. Seasonal plankton dynamics along a cross-shelf gradient. Proc. Roy. Soc. London B 273, 2831–2838. http://dx.doi.org/10.1098/rspb.2006.3658.
Sverdrup, H.U., 1953. On conditions for the vernal blooming of phytoplankton. Journal du Conseil International pour l'Exploration de la Mer 18, 287–295.
Torrence, C., Compo, G.P., 1998. A practical guide to wavelet analysis. Bull. Am. Meteorol. Soc. 79, 61–78. http://dx.doi.org/10.1175/1520-0477(1998) 079, 0061:APGTWA > 2.0.CO;2.
Van Haren, H., Mills, D.K., Wetsteyn, L.P.M.J., 1998. Detailed observations of the phytoplankton spring bloom in the stratifying central North Sea. J. Mar. Res. 56, 655–680. http://dx.doi.org/10.1357/002224098765213621.
Weston, K., Fernand, L., Mills, D.K., Delahunty, R., Brown, J., 2005. Primary production in the deep chlorophyll maximum of the central North Sea. J. Plankton Res. 27, 909–922.
Weston, K., Greenwood, N., Fernand, L., Pearce, D.J., Sivyer, D.B., 2008. Environmental controls on phytoplankton community composition in the Thames plume, U.K. J. Sea Res. 60, 246–254. http://dx.doi.org/10.1016/j.seares.2008.09.003.
Winder, M., Cloern, J.E., 2010. Annual cycles of phytoplankton biomass. Philos. Trans. Roy. Soc. B-Biol. Sci. 365, 3215–3226. http://dx.doi.org/10.1098/rstb.2010.0125.
Wood, S.N., 2013. On *p*-values for smooth components of an extended generalized additive model. Biometrika 100, 221–228.
Wood, S., 2006. Generalized Additive Models: An Introduction with R. CRC Press.